The shifted reflective boundary for the study of two-phase systems with molecular dynamics simulations

William d'Haeseleer, Geert van den Branden, Martine Baelmans

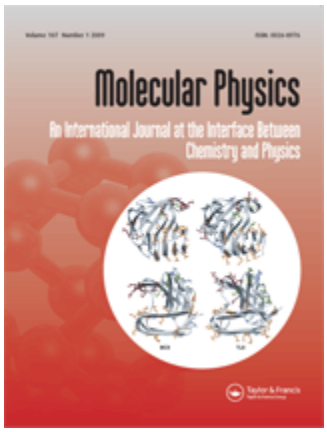

The shifted reflective boundary for the study of two-phase systems with molecular dynamics simulations

Journal:	*Molecular Physics*
Manuscript ID:	TMPH-2007-0228.R1
Manuscript Type:	Full Paper
Date Submitted by the Author:	21-Nov-2007
Complete List of Authors:	D'haeseleer, William; University of Leuven, K.U.Leuven, Department of Mechanical Engineering Van den Branden, Geert; University of Leuven, K.U.Leuven, Department of Mechanical Engineering Baelmans, Martine; University of Leuven K.U.Leuven, Department of Mechanical Engineering
Keywords:	Molecular Dynamics, Boundary Condition, Two-Phase Systems

Submitted to Molecular Physics

The shifted reflective boundary for the study of two-phase systems with molecular dynamics simulations

Author Information

Geert Van den Branden

University of Leuven, K.U.Leuven,
Division of Applied Mechanics and Energy Conversion
Celestijnenlaan 300A, B-3001 Leuven, Belgium
Tel. +32 16 32 25 08
Fax +32 16 32 29 85
Email: geert.vandenbranden@mech.kuleuven.be

Martine Baelmans

University of Leuven, K.U.Leuven,
Division of Applied Mechanics and Energy Conversion
Celestijnenlaan 300A, B-3001 Leuven, Belgium
Tel. +32 16 32 25 11
Fax +32 16 32 29 85
Email: martine.baelmans@mech.kuleuven.be

William D'haeseleer

University of Leuven, K.U.Leuven,
Division of Applied Mechanics and Energy Conversion
Celestijnenlaan 300A, B-3001 Leuven, Belgium
Tel. +32 16 32 25 11
Fax +32 16 32 29 85
Email: william.dhaeseleer@mech.kuleuven.be

Submitted to Molecular Physics

The shifted reflective boundary for the study of two-phase systems with molecular dynamics simulations

G. VAN DEN BRANDEN, M. BAELMANS and W. D'HAESELEER*

University of Leuven, K.U.Leuven, Division of Applied Mechanics and Energy Conversion
Celestijnenlaan 300A, B-3001 Leuven, Belgium

When studying fluids with molecular dynamics simulations, periodic boundaries are usually used to model an infinite bulk fluid surrounding the primary cell. For homogeneous systems this is, as a rule, the most appropriate way. For inhomogeneous systems, e.g. systems with a fluid-vapour interface, periodic boundaries suffer some disadvantages. Therefore, an alternative for periodic boundaries, called shifted reflective boundary, is proposed for modelling such systems. From a computational point of view, this type of boundary is not more difficult to implement than periodic boundaries. It is shown that the shifted reflective boundary results in a stable spatial fluid-vapour configuration with one fluid-vapour interface, while retrieving the same numerical results for thermodynamic properties, e.g. the surface tension, as molecular dynamics simulations with periodic boundaries. Molecular dynamics simulations with shifted reflective boundaries also need fewer particles than corresponding simulations with periodic boundaries.

Keywords: Molecular Dynamics; Boundary Condition; Two-Phase Systems

* Corresponding author. Email: william.dhaeseleer@mech.kuleuven.be

1. Introduction

Molecular Dynamics (MD) simulation is a powerful and instructive numerical tool to study thermodynamic and kinetic processes in great detail, for i.a. the fluid-vapour interactions at the interface of a two-phase system. MD simulations are performed on a system of relatively small size in comparison with real thermodynamic systems (e.g. a system of 10^3 versus 10^{23} particles), thereby, nevertheless leading to statistically significant results. To model the world surrounding the MD system, different types of boundary conditions can be used (periodic, free, reflective), see [1]. For the study of single-phase systems, classical Periodic Boundaries (PB) are very appropriate. Unfortunately, PB conditions for two-phase vapour-liquid systems are not always appropriate to study the molecular processes at the interface. For that purpose, we would prefer a single flat interface remaining fixed in space. Therefore, we present a new type of boundary condition which is particularly adapted to study the two-phase vapour-liquid interface.

As a demonstration, Figure 1 (a) shows the results of a small MD simulation of Argon atoms in a system with a cubic cell with PB conditions. The forces between the Argon atoms are derived from a Lennard-Jones (LJ) potential. It is clear from this figure that the minimalisation of the free energy will result in a spherical-like interface. The position of the interface between the vapour and the liquid phase is not fixed since the droplet of liquid will wander throughout the system cell, and thereby possibly pass the PBs of the cell.

The spherical shape of the interface can be avoided by using a cell with a large aspect ratio. Minimalisation of the intermolecular energy by the system will result in a flat film of liquid surrounded by a vapour phase. Figure 1 (b) shows the result for a MD simulation of

Argon atoms in such a cell. This geometry of a double planar fluid-vapour interface has been used by among others [2-5] for their study of the interfacial properties of a LJ fluid. In principle, the liquid film will continue to randomly oscillate up and down the cell. Thermodynamic properties as pressure, temperature and surface tension can be calculated straightforward irrespective of these oscillations. For properties as the fluid and vapour densities, the presence of the oscillations can be sidestepped by monitoring the evolution of the centre of mass and continuously shifting the centre of mass of the cell back to a fixed position during the simulation. However, below we present a simpler and less intervening technique, whereby the fluid-vapour configuration is fixed through a specially adapted boundary condition the Shifted Reflective Boundary (SRB); which was developed to permit in a following stage the easy calculation of time correlation functions and pair-wise density functions at the interface.

The paper is organized as follows. In Section 2, we introduce the Shifted Reflective Boundary (SRB). Furthermore, in this section, the computational implications of the calculation of the intermolecular forces with SRBs are presented. In Section 3, we demonstrate some results of MD simulations using the SRBs: firstly, the individual behaviour of a particle in the vicinity of a SRB during a MD simulation; secondly, the collective behaviour of a two-phase system in a cell with a SRB compared to a corresponding MD simulation with PBs, thirdly, a quantitative comparison of two-phase MD calculations with SRBs and PBs for a range of temperature; fourthly the influence of the number of particles on the calculated surface tension in MD simulations with SRBs and PBs; finally, the stability of the fluid-vapour configuration in a MD simulation with a SRB.

2. Shifted reflective boundary condition

2.1. Rationale and principle

The purpose of the SRB is to model a system with one single fluid-vapour interface, whereby this interface, apart from naturally occurring variations, should remain fixed in space. This can be obtained when the boundary condition of one of the walls models the presence of an infinitely large unperturbed fluid phase. The fluid molecules in the cell will preferentially be present next to this boundary, since that position minimises their intermolecular energy. This way, the fluid phase stays attached to that boundary and, consequently, the vapour-liquid interface remains fixed in space.

The modelling of a liquid boundary condition, however, is not trivial. Indeed, a stationary attractive intermolecular force will not accurately predict the liquid behaviour. On the contrary, to model the liquid boundary condition, a dynamically varying force is needed to take into account the movement of molecules in a liquid. This movement of molecules is the most faithfully and the most easily modelled by using the liquid molecules already present in the primary cell during the MD simulations. This is the principle of the SRB condition presented in this paper.

2.2. Definition of the SRB

Like systems with PBs, a system with a SRB makes use of image cells but these image cells are defined in a different way. Figure 2 shows the primary cell of a system with a SRB at the bottom wall surrounded by its image cells. In the x- and y-direction the primary cell (0,0) is surrounded by classical periodic image cells (i,j). At the bottom, however, the primary cell is surrounded by shifted reflective image cells (i,j)*, these are specularly

reflected mirror images of the primary cell (and its periodic image cells) with the bottom wall serving as the plane of reflection, but whereby the image cell is simultaneously shifted in the x- and y-direction by a distance s_x and s_y respectively. (The shift s_y and the periodic repetition of cells in the y-direction are not visible in Figure 2.)

Defined as such, the SRB results, for particles i in the vicinity of the SRB, in intermolecular interactions with particles j^* which are image particles of particles j that are also situated in the vicinity of the SRB. Although the SRB condition has been defined to model a 'liquid boundary condition' to obtain a stable configuration of liquid and vapour, this boundary condition makes no a priori assumptions about the particle configuration and behaviour in the vicinity of the boundary, and, hence, it can also be used for other types of MD simulations, e.g. single-phase systems.

The boundary condition at the opposite boundary of a SRB, i.e. the top wall in Figure 2, can be a reflective boundary or another SRB, but not a PB, since this last boundary condition always has to be implemented in pairs. The boundary conditions in the x- and y-direction are restricted to PBs. For the purpose of clarity, a system with a simple reflective boundary condition at the top wall is used to illustrate the SRB in Figure 2. The shift (s_x,s_y) could in principle be freely chosen, but the most appropriate choice is a shift equal to half the dimensions of the primary cell in the x- and y-direction, $(s_x,s_y) = (\Delta x/2,\Delta y/2)$. From the definition of the SRB, it results that the x- and y-components of the velocities of a particle and it SRB image particle are equal, but that their z-component are opposite in sign.

2.3. Re-insertion of particles crossing a SRB

When, during a MD simulation, a particle happens to cross a SRB, it is re-inserted into the primary cell in the way shown in Figure 3. The z-component of the position of the particle remains unchanged, while the x- and y-component are increased by $\Delta x/2$ and $\Delta y/2$, respectively. Simultaneously, the z-component of the velocity of the particle is reversed while the x- and y-components remain unchanged; i.e., the moment a particle leaves the primary cell, it reappears with the position and velocity of its image particle. The particle loses or gains neither kinetic nor intermolecular energy in this procedure, as will be shown in Section 3.1. It is not necessary to perform the re-insertion transformation at the exact moment of boundary crossing. Particles can leave the primary cell during a calculation step, the moment a particle crosses the boundary, its image particle will enter the primary cell and particle and image particle temporarily switch roles.

However, as an alternative to the procedure described above, to determine the velocity of a re-inserted particle, the SRB permits to impose a wall temperature T, by randomly choosing the velocity of the re-inserted particle from a Maxwell-Boltzmann distribution at temperature T, see [6]. Since, with SRBs and in contrast to PBs, the opposite walls of a cell do not necessary have to be identical, the temperature at the SRB top wall and the SRB bottom wall can be different and a temperature gradient can be imposed.

2.4. Intermolecular force and cut-off radius

It is well known that, for systems with PBs, there will be intermolecular interactions between a particle i and its own image particles, if the intermolecular force has a long range with respect to the dimensions of the primary cell. In addition, there might be

intermolecular interactions between a particle *i* and several image particles of the same particle *j*. The same is true for systems with SRBs. Since the motion of a particle and the motion of its image particles are highly correlated, these kinds of interactions can hardly be considered to be realistic and have to be avoided in MD simulations.

In this section, we will determine the minimum dimensions necessary to achieve this, for a primary cell with a SRB as a function of the cut-off radius σ_c of the intermolecular forces, i.e. the distance between two molecules above which no intermolecular interaction occurs. For matters of comparison, we start with the relation between the minimum dimensions of the primary cell and the cut-off radius σ_c for a system with PBs.

For a primary cell with dimensions Δx, Δy and Δz, and with PBs, it is easy to show that no particle *i* interacts with periodic image particles *i*' of the particle *i* itself, if

$$\sigma_c < \min(\Delta x, \Delta y, \Delta z) . \tag{1}$$

In addition, each particle *i* only interacts with one single periodic image particle *j*' of particle *j* (or particle *j* itself), if, see [7],

$$\sigma_c < \min(\Delta x/2, \Delta y/2, \Delta z/2) . \tag{2}$$

For systems with a SRB at the bottom (or top) of a primary cell, the conditions imposed on the dimensions of the primary cell are more severe. No particle *i* interacts with a shifted reflective image particles *i** of the particle *i* itself, if

$$\sigma_c < \left((\Delta x/2)^2 + (\Delta y/2)^2\right)^{1/2} . \tag{3}$$

To impose that each particle *i* only interacts with the shifted reflective image particle *j** of particle *j* or one of the periodic image particles *j*' of particle *j* (including particle *j* itself), it is necessary that

The shifted reflective boundary

$$\sigma_c < \left((\Delta x/4)^2 + (\Delta y/4)^2\right)^{1/2}. \quad (4)$$

If there is a SRB at the top and bottom of the system, then there is the additional condition that

$$\sigma_c < \Delta z. \quad (5)$$

This last condition is only relevant for very wide and flat primary cells. For systems with a square base of the primary cell, i.e. $\Delta x = \Delta y$, comparison between the corresponding conditions for systems with PBs of equations (1) and (2), and the corresponding conditions for systems with SRBs of equations (3) and (4), show that the primary cell needs to be a factor $\sqrt{2}$ larger in the case of the SRBs to avoid the undesirable particle interactions. As such, this is a disadvantage of the use of a SRB. It has to be noted, however, that when neglecting the most stringent condition of equation (4), the undesirable intermolecular interactions only occurs for particles close to the SRB. No undesirable interactions can occur for particles at distances larger than the distance d_{max} from the SRB, with

$$d_{\max} = \left(\sigma_c^2 - (\Delta x/4)^2 - (\Delta y/4)^2\right)^{1/2}. \quad (6)$$

As such, only a very small fraction of the total number of particle interactions are to be considered unrealistic, all of which situated near boundary where the SRB has been applied. If equation (2) holds, in the worst case, only a fraction of less than 12% from all the intermolecular interactions between particles situated at a distance from the SRB smaller than $d_{\max}$ has to be considered as unrealistic.

2.5. Calculation of the intermolecular forces with shifted reflective boundaries

Due to the symmetry properties of the SRB condition with a shift of half a cell, the calculation of the intermolecular forces between particles and shifted reflected image

particles can be greatly simplified. When particle i interacts with an image particle j^* through an intermolecular force F_{ij*}, then there is also an intermolecular force F_{ji*} between a particle j due to an image particle i^* of equal magnitude. The orientation of both intermolecular forces however is slightly different,

$$F_{ij*} = F_{ji*}, \tag{7}$$

and

$$F_{ij*,x} = -F_{ji*,x} \ , \ F_{ij*,y} = -F_{ji*,y} \ , \ F_{ij*,z} = +F_{ji*,z} \ . \tag{8}$$

2.6. Comparison periodic boundaries and shifted reflective boundaries

In the previous sections, we have shown that SRBs with a shift of half a cell possess many symmetry properties similar to PBs. The result is that the MD simulations with SRBs require no extra computational effort compared to MD simulations with PBs. Table 1 gives an overview of the similarities and differences for a system with PBs and a system with a SRB at the bottom wall of the primary cell. In the following section, we will show that the SRB possesses all the properties we described above. It will also become clear that the SRB is a kind of hybrid boundary condition having features in common with both PBs and classical reflective boundaries.

2.7. The SRB and the finite size effect

It has been observed [8] that for small systems with PBs, the values of thermodynamic properties as pressure and surface tension are sensitive to cell geometry and size. For increasing cell dimensions, the value of the observed variables converges periodically or monotonically towards the thermodynamic value. Using large cells (with more particles) can resolve this problem, but at the cost of larger computational time. Since SRBs are periodic in nature in the x and y-direction, it can be expected that they suffer from the

same finite size effect. However, as will be shown in Section 3.4, for a cell of fixed size, a system with SRBs needs fewer particles to obtain a stable fluid-vapour interface than a system with PBs. Hence, for a fixed number of particles, larger cells can be used.

3. Results of MD simulations with a shifted reflective boundary

3.1. Behaviour of a particle in the vicinity of a shifted reflective boundary

In Section 2, we defined the SRB. In this section, we illustrate the effect of the SRB on the behaviour of a single particle in the vicinity of a SRB during MD simulation A. The parameters and results of this and all subsequent MD simulations are conventionally rendered dimensionless using reduced Lennard-Jones units, see among others [5], length $z^* = z/\sigma$, energy $e^* = e/\varepsilon$, time $t^* = t\sqrt{\varepsilon/m}/\sigma$, temperature $T^* = k_B T/\varepsilon$, pressure $p^* = p\sigma^3/\varepsilon$, surface tension $\gamma^* = \gamma\sigma^2/\varepsilon$, velocity $v^* = v\sqrt{m/\varepsilon}$. The system consists of 3685 LJ particles in a cell of dimensions 14.1 × 14.1 × 70.5. The boundaries the in x- and y-directions are PBs. In the z-direction, at the bottom wall (z = -34.78), a SRB is implemented, whereas at the top wall (z = +34.78) a reflective boundary is present. The temperature of the system is 0.98 using Andersen's thermostat [8]. The cut-off ratio used for this and all subsequent calculations is 3.45 σ. Table 2 gives an overview of the principal parameters of the MD simulations.

Figure 4 shows the evolution of the x- and z-components of the position and the velocity of a single particle during MD simulation A. The y-component is not depicted but the evolution of this component is similar to that of the x-component. Although the duration of this MD simulation was much longer, the time span of the plotted results is limited to 6.84 in order not to overload the figure. In Figure 4 (a) and (b), the boundaries of the primary

cell are indicated with a dash-dot line. The particle crosses the SRB at the bottom of the cell (z = -34.78) on several occasions. The different instances of boundary crossings are marked with the symbol ×.

Figure 4 (a) and Figure 4 (c) show the evolution of the x-components of the position and the velocity of the particle, respectively. Each boundary crossing involves a discontinuity in the x-component of the position of the particle, whereby the particle is shifted by half a cell width, see Figure 4 (a). The x-component of the velocity, however, remains unchanged when crossing a SRB, see Figure 4 (c).

The evolution of the z-components of the position and the velocity is completely different, see Figure 4 (b) and Figure 4 (d), respectively. There are no discontinuities present in the z-component of the position of the particle, see Figure 4 (b), while the sign of the z-component of the velocity is reversed every time the particle crosses the SRB, see Figure 4 (d). Notwithstanding the seemingly discontinuous behaviour of the particle when crossing a SRB, the particle experiences a smooth transition, as was mentioned in Section 2.2. This can be seen in Figure 5, where the evolution of the kinetic and intermolecular energy of the same particle is depicted, again with the boundary crossings marked with the symbol ×. The evolution of the kinetic and the intermolecular energy are both continuous, meaning that no energy is lost or gained when crossing the SRB.

For clarity, during this MD simulation the particle is shifted and the velocity is reversed at exactly the moment of the boundary crossing. As previously stated, this is not compulsory.

3.2. Molecular dynamics simulation of a system of LJ particles

In this section, we will present a typical result of a two-phase MD simulation with a SRB condition and compare it with the results of a two-phase MD simulation of a system with PBs. For MD simulation B, with the SRB, the set-up is the same as MD simulation A of the previous section. For MD simulation C, PBs are implemented in the z-direction instead of SRBs, see also Table 2.

Figure 6 (a) shows the position of the particles at the end of MD simulation B. As we envisaged in Section 2, most particles are present in the liquid phase at the bottom of the cell, due to the SRB situated at $z = -\Delta z/2$.

Figure 7 (a) shows the position of the particles at the end of MD simulation C. The result is typical for a two-phase system in a cell with PBs. Although the fluid phase was initially perfectly centred, due to the fluctuations during the MD simulations, it has slowly moved upwards.

Very interesting is the comparison of the vertical distribution of the particles as a function of their kinetic and intermolecular energy for MD simulation B with a SRB, see Figure 6 (b) and (c), and the same distribution for MD simulation C for PBs, see Figure 7 (b) and (c). The two different phases are very distinctively recognisable in both figures, firstly, due to the fact that the fluid phase has a much larger density than the vapour phase and, secondly, because particles in the fluid phase, on average, have a much larger intermolecular energy (in the sense of a larger absolute value, although the attractive intermolecular forces are conventionally considered as being negative). Figure 6 also shows that the presence of a SRB does not change the properties of the fluid phase in its

vicinity. The fluid phase behaves as if it is bounded at the bottom of the primary cell by an infinite bulk fluid.

The number of particles in both MD simulations being identical, it is clear that the number of particles at the interface between vapour and fluid is twice as large in the MD simulation with PBs (Figure 7) compared to the MD simulation with a SRB (Figure 6) and that, consequently, the number of bulk fluid particles is larger in MD simulations with a SRB. If the number of particles in the MD simulation is too small, no bulk fluid phase will develop, and the results will not be representative for real fluid-vapour systems. As a consequence, MD simulations with a SRB require a lower number of particles than corresponding MD simulations with PBs. This will be demonstrated in detail in the next section.

3.3. Comparison of two-phase systems with SRBs and systems with PBs

In this Section, the results of MD simulations of two-phase systems with SRBs and PBS are compared for temperatures T^* ranging from 0.65 to 1.05, see Table 2 for the principal parameters of the different MD simulations. For the MD simulations with PBs (MD simulations E1-E9), after each time step, the centre of mass of the particles was reshifted to the geometrical centre of the cell. For systems with SRBs (MD simulations D1-D9), no measures had to be taken to keep the fluid phase fixed at the bottom of the cell. Figure 8 shows the results of the MD calculations for both types of boundary conditions as a function of temperature. Figure 8 (a) en (b) show the fluid and vapour densities of the two-phase state, respectively. Figure 8 (c) shows the corresponding saturation pressure and Figure 8 (d) the surface tension. The surface tension is classically calculated as the

difference of the normal and the transverse component of the pressure, see among others [10]. The results for the MD calculation with SRBs (solid line) correspond well with the results for the MD calculation with PBs (dashed line) over the whole range of temperatures. The presence of the SRBs instead of the classical PBs does not change the thermodynamic properties of the system, as was required.

3.4. Effect of the number of particles

In Section 2, it was stated that a SRB has the advantage that it will provide statistically significant results even with fewer particles in the MD simulation than a corresponding simulation with PB conditions and this due to the fact that only one interface is present. In this section, the evolution of the surface tension for different MD simulations is presented as a function of the number of particles N. The basic set-up is identical as in the previous sections, with the sole exception of the total number of particles, the dimensions of the cell are constant for all simulations, irrespective of the number of particles. For the MD simulations F1 through F8, the boundary in the z-direction at the bottom of the primary cell (z = -34.78) is a SRB, the boundary at the top (z = -34.78) is a reflective boundary. For MD simulation G1 through G8, the boundaries in the z-direction are PBs. The number of particles N in the MD simulations varies for MD simulations F1 through F8 (and correspondingly G1 through G8), and equals 500, 750, 875, 1000, 1125, 1250, 1500 and 2000, respectively, see Table 2 for more details on MD simulations F and G . The initial configuration of the particles was constructed in such a way that a liquid and vapour phase were present. The particle distribution for the liquid and vapour phase was taken from a previous MD simulation at the same temperature. Figure 9 shows the surface tension as a

function of the number of particles *N*. For large number of particles *N*, both systems with SRBs and PBS obtain the same values for the surface tension, corresponding with the results given by [11]. On the other hand, for systems with small values of *N*, and notwithstanding the careful preparation of the initial configuration, the liquid phase breaks up during the MD calculation, resulting in a homogeneous phase and, consequently, zero surface tension. However, it is clear, from this figure, that fewer particles are required for an accurate result with a SRB than in case of a system with PBs.

3.5. Stability of a system with a shifted reflective boundary

When a SRB is present at one of the boundaries of a primary cell, the fluid phase of a two-phase fluid-vapour system will reside preferentially at the SRB. To illustrate this, the evolution of the spatial configuration a two-phase fluid-vapour system is calculated for a system with a SRB at the bottom of the primary cell (MD simulation H). The initial condition of the system is a fluid phase centred in the middle of the cell surrounded on top and bottom by a vapour phase in equilibrium with this fluid phase. This initial condition was the result of a previous MD simulation with a PB. Equilibrium between the vapour and fluid phase was attained, while actively fixing the position of the fluid droplet by continuously resetting the centre of mass of the system to the middle of the cell. The initial state is shown in Figure 10 (a). The system consists of 3687 particles in a primary cell of dimensions $17.4 \times 17.4 \times 43.48$. The boundary conditions in the x- and y-directions are PB conditions. The temperature of the system is 0.87 using Anderson's thermostat.

During MD simulation H, the fluid phase was not centred. Due to fluctuations caused by the Andersen's thermostat the system is expected to wander up and down the primary cell,

eventually reaching the SRB at the bottom of the cell. The time it would take to reach the bottom of the primary cell, solely as a result of statistical fluctuations, would be, according to MD measures, astronomical. Since we are mainly interested in the fluid phase interacting with the SRB, we give the particles, between a time $t = 228$ and $t = 388$, through the thermalisation process, on average a little downwards velocity of 0.64. This push does not incriminate the results of this MD simulation, since the fluid phase would eventually have reached the SRB at the bottom of the cell at some point in time, though probably with a lower mean velocity. At time $t = 388$, the fluid droplet approaches the bottom of the cell, see Figure 10 (b), and no downwards push is further on applied. When the MD simulation would have employed a simple reflective boundary, the fluid phase would have bounced back upwards. With a PB, the fluid phase would have continued to go downwards and would have reappeared at the top of the cell. With the SRB, the fluid phase stays attached at the bottom of the cell, as can be seen from Figure 10 (c).

Figure 11 depicts the evolution of the vertical position of the centre of mass, the average vertical velocity and the total intermolecular energy of the system as a function of time. In the first stage of the simulation (from $t = 0$ till $t = 228$), without the downward push, the vertical velocity of the system fluctuates around zero and, hence, the vertical position of the centre of mass does not change significantly. The intermolecular energy, apart from some naturally occurring fluctuations, remains constant.

During the second stage of the simulation (from $t = 228$ till $t = 388$), with the downward push, the z-component of the average velocity of the system fluctuates, as expected, around the value -0.64. Accordingly, the z-component of the position of the centre of mass of the system decreases, and the fluid-phase, in which most particles reside, is moving

downwards. After a while, the intermolecular energy of the system starts to decrease, since fluid particles begin to interact with SRB image particles and the LJ potential at long intermolecular distances is attractive.

During the third stage of the simulation (from $t = 388$ till $t = 730$), again without downward push, the fluid phase first starts to slow down in its downward movement. This is due to the reflective character of the SRB. Particles crossing the SRB are re-inserted into the primary cell with an upwards velocity, thereby decreasing the overall downward velocity of the system. However, when the fluid phase further approaches the SRB, the attractive intermolecular forces of SRB image particles on the fluid phase gain the upper hand and accelerate the fluid phase downwards to the SRB. When the fluid phase crosses the SRB, many particles are re-inserted with an upwards velocity, and the downward movement is abruptly halted, see Figure 11 (b). From this moment one the average vertical velocity fluctuates around a value of zero and the vertical position of the centre of mass fluctuates around its equilibrium position, with the fluid phase attached to the SRB, see Figure 11 (a). At the start of the third stage, when the fluid-phase is still moving downwards, the intermolecular energy continues to decrease, see Figure 11 (c). However, the moment the fluid-phase reaches the SRB with a large downward velocity, the particles and image particles approach each other at relatively short intermolecular distances, at which the LJ intermolecular forces become repulsive, resulting in an increase in intermolecular energy and a further halt to the downwards movement. As soon as this short transitional phase ends, the particles and image particles resettle and, through their mutual attractive interactions, the intermolecular energy of the system strongly decreases.

The shifted reflective boundary

The low intermolecular energy signifies that more particles are *bulk* liquid particles with a lower intermolecular energy, when the fluid phase resides at the bottom of the cell, and consequently in the vicinity of the SRB, than when the fluid phase resides away from the SRB. In fact, when the fluid phase is situated at the bottom of the cell, there is only one single fluid-vapour interface left of the two interfaces present at the start of the simulation. The particles at the bottom interface have all been transformed into bulk fluid particles, hence decreasing the intermolecular energy.

Figure 11 shows that the randomly occurring fluctuations of the intermolecular energy are much smaller than the difference in intermolecular energy between a fluid phase which is detached from a SRB and a fluid phase which is attached to a SRB. This means that the probability that the fluid phase detaches from the SRB due to statistical thermal fluctuations is very small and that the system will preferentially resides in the part of phase-space with the fluid phase attached to the SRB.

The stability of the final configuration, as shown in Figure 10, can be further quantified when looking at the difference in average total intermolecular energy between the two-phase system with two interfaces in the first stage of the simulation (from $t = 0$ to 388) and the two-phase system with one interface in the final stage of the simulation (from $t = 502$ to 730). The average of the total intermolecular energy of the system with two interfaces is -16 685±42, the average of the total intermolecular energy of the system with one interface is -17 606±36, a difference of 922±55. This value has to be compared with the variance around the total intermolecular energy of the system with one interface, which equals 139. If we assume that the accessible states are Gaussian distributed around the most probable

state, see [13], then the system has only a probability of approximately one in 6×10^{10} to reside in a state with a detached liquid phase.

This has two consequences. Firstly, for a system with a SRB, the initial condition of a MD simulation is very important, more than with PBs, in order to keep the simulation within realistic computational times. Indeed, although a fluid phase at the centre or at the top of the primary cell is not excluded, the fluid phase at the bottom of the cell is much more probable and therefore much more representative of all possible systems in phase space. Secondly, since the chance of detaching from the SRB is very small, there is no need to actively monitor and fix the position of the fluid phase in the primary cell, as is usually done during MD simulations employing PBs. With a SRB, the fluid phase stays fixed in a very natural way. The height of the fluid-vapour interface, though, can vary a bit through statistical fluctuations, as it would be expected. This feature was one of the main reasons for the development of the SRB.

4. Conclusions

In this paper, we have presented a special type of boundary condition: the shifted reflective boundary condition for molecular dynamics simulations of systems with a vapour-liquid interface. Notwithstanding the seemingly artificial character of this boundary condition, this boundary condition is clearly capable of calculating the properties of a two-phase system. Compared to PBs, the shifted reflective boundary has the advantage that fewer particles are situated at the fluid-vapour interface, thereby reducing the minimum number of particles needed in a two-phase simulation. Secondly, since in a system with a shifted

reflective boundary the fluid phase stays attached at the shifted reflective boundary, the detailed study of the interface properties and processes can be greatly facilitated.

References

[1] Daan Frenkel and Berend Smit, Understanding Molecular Simulation, Academic Press, San Diego (2002).

[2] M.J.P. Nijmeijer, A.F. Bakker, C. Bruin, J. Chem. Phys., **89**, 3789 (1988).

[3] Andrij Trokhymchuk, José Alejandre, J. Chem. Phys., **111**, 8510 (1999).

[4] Daniel Duque, Lourdes F. Vega, J. Chem. Phys. **121**, 8611 (2004).

[5] Jadran Vrabec, Gaurav Kular Kedia, Guido Fuchs, Hans Hasse, Mol. Physics., **104**, 1509 (2006).

[6] Alexander Tenenbaum, Giovanni Ciccotti, Renato Gallico, Phys. Rev. A., **25**, 2778 (1982).

[7] Doros N. Theodorou and Ulrich W. Suter, J. Chem. Phys. **82**, 955 (1985)

[8] Minerva González-Melchor, Pedro Orea, Jorge López-Lemus, Fernando Bresem, José Alejandre, J. Chem. Phys. 122,094503 (2005)

[9] Andersen, H.C., J. Chem. Phys., **72**, 2384 (1980)

[10] John G. Kirkwood, Frank. P. Buff, J. Chem. Phys., **17**, 338 (1949)

[11] V.G. Baidakov, G.G. Chernykh, S.P. Protsenko, Chem. Phys. Lett., **321**, 315 (2000).

[12] J.M. Haile, Molecular Dynamics Simulation, John Wiley & Sons, New York (1992).

[13] F. Reif, Fundamentals of Statistical and Thermal Physics, McGraw-Hill, New York (1965).

Table 1: Comparison of Periodic and Shifted Reflective Boundary Condition

	Periodic Boundary	Shifted Reflective Boundary
transformation rule position image particle	$x \rightarrow x + m\,\Delta x$ $y \rightarrow y + n\,\Delta y$ $z \rightarrow z + p\,\Delta z$ m, n, p any integer number	$x \rightarrow x + \Delta x/2 + m\,\Delta x$ $y \rightarrow y + \Delta y/2 + n\,\Delta y$ $z \rightarrow - \Delta z - z$ m, n any integer number
transformation rule velocity image particle	$v_x \rightarrow v_x$ $v_y \rightarrow v_y$ $v_z \rightarrow v_z$	$v_x \rightarrow v_x$ $v_y \rightarrow v_y$ $v_z \rightarrow - v_z$
relationship between the intermolecular force F_{ij*} on particle i due to nearest image particle of j and the intermolecular force F_{ji*} on particle j due to nearest image particle of i	$F_{x,ij*} = - F_{x,ji*}$ $F_{y,ij*} = - F_{y,ji*}$ $F_{z,ij*} = - F_{z,ji*}$	$F_{x,ij*} = - F_{x,ji*}$ $F_{y,ij*} = - F_{y,ji*}$ $F_{z,ij*} = + F_{z,ji*}$

The shifted reflective boundary

Table 2 Overview of the principal parameters of the MD simulations. All values are in reduced Lennard-Jones units. The boundary condition indicated is the boundary condition in the z-direction. The boundary conditions in the x- and y-direction are always PBs.

Name	Dimensions $\Delta x^* \times \Delta y^* \times \Delta z^*$	Boundary condition	Temperature	Number of Particles
A	14.1 × 14.1 × 70.5	SRB	0.98	3685
B	14.1 × 14.1 × 70.5	SRB	0.98	3685
C	14.1 × 14.1 × 70.5	PB	0.98	3685
D1-D9	17.4 × 17.4 × 43.48	SRB	0.65, 0.7, 0,75, 0.8, 0.85, 0.9, 0.95, 1.0, 1.05	3685
E1-E9	17.4 × 17.4 × 43.48	PB	0.65, 0.7, 0,75, 0.8, 0.85, 0.9, 0.95, 1.0, 1.05	3685
F1-F8	14.1 × 14.1 × 70.5	SRB	0.98	500, 750, 875, 1000, 1125, 1250, 1500, 2000
G1-G8	14.1 × 14.1 × 70.5	PB	0.98	500, 750, 875, 1000, 1125, 1250, 1500, 2000
H	17.4 × 17.4 × 43.48	SRB	0.87	3687

List of Figure Captions

Figure 1: x-z –projection of Argon atoms particles in a MD simulation in a cubic cell with PB conditions (a) and x-z –projection of Argon atoms in a MD simulation in a cuboid cell with PB conditions (b).

Figure 2: Lay-out of the primary cell and the image cells for the SRB condition (x-z view, the y-axis is perpendicular to the plane of the figure).

Figure 3: Re-insertion of particles in case of a SRB at the bottom wall, a simple reflective boundary at the top wall and a PB at the side walls: (a) before re-insertion, (b) after re-insertion.

Figure 4: Evolution of the x-component (a) and z-component (b) of the position and of the x-component (c) and z-component (d) of the velocity as a function of time of a particle in the vicinity of the SRB for MD simulation A.

Figure 5: Evolution of the kinetic (a) and intermolecular (b) energy of a particle in the vicinity of the SRB condition for MD simulation A.

Figure 6: Results at the end of MD simulation B with a SRB at the bottom of the cell: (a) x-component of the position of the particles s a function of the z-position, (b) intermolecular energy of the particles as a function of the z-position, (c) kinetic energy of the particles as a function of the z-position.

Figure 7: Results at the end of MD simulation C with a PB at the top and bottom of the cell: (a) x-component of the position of the particles s a function of the z-position, (b)

intermolecular energy of the particles as a function of the z-position, (c) kinetic energy of the particles as a function of the z-position.

Figure 8: Evolution of the liquid density (a), the vapour density (b), the saturation pressure (c) and the surface tension (d) as a function of temperature of a two-phase system, for MD simulations D1-D9 with a SRB (solid line) and for MD simulations E1-E9 with PBs (dashed line). The error bars indicate the 95% confidence interval, see [12]. All values are in reduced Lennard-Jones units.

Figure 9: Evolution of the surface tension as a function of the number of particles for MD simulations F1-F8 with a SRB (solid line) and for MD simulations G1-G8 with PBs (dashed line). The error bars indicate the 95% confidence interval, see [11].

Figure 10: x-z-view of the initial state (a) at t = 0, of the intermediate state (b) at t = 388 and of the end state (c) at t = 730 of the particles in a two-phase system with a SRB condition at the bottom wall for MD simulation H.

Figure 11: Evolution of the z-component of the position of the centre of mass (a), average vertical velocity (b) and total intermolecular energy (c) of the particles in a two-phase system with a SRB for MD simulation H.

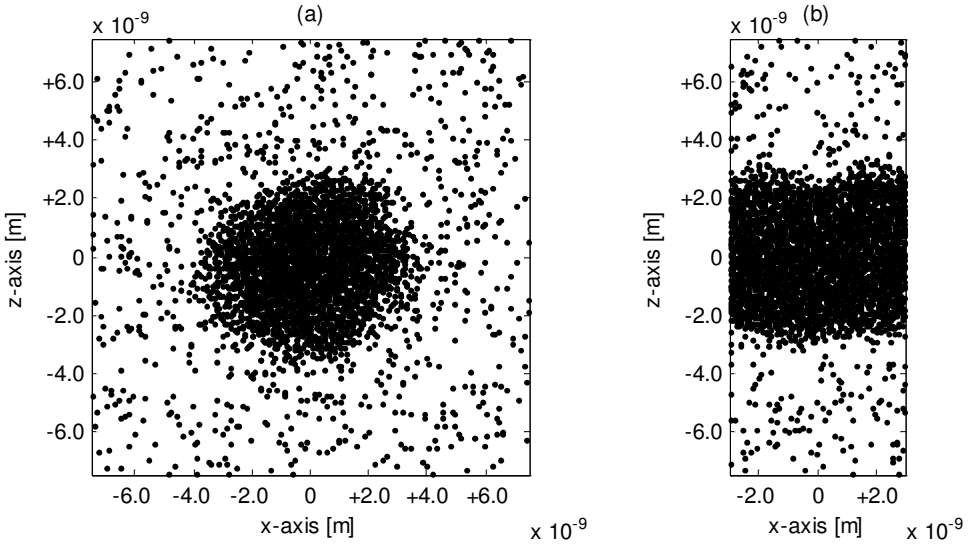

Figure 1: x-z –projection of Argon atoms particles in a MD simulation in a cubic cell with PB conditions (a) and x-z –projection of Argon atoms in a MD simulation in a cuboid cell with PB conditions (b).

The shifted reflective boundary

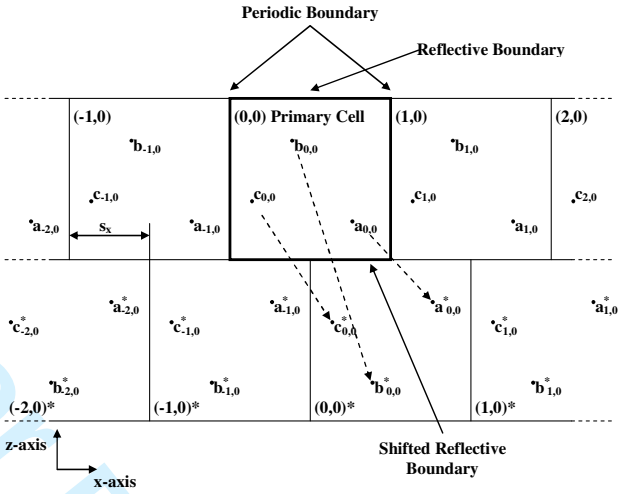

Figure 2: Lay-out of the primary cell and the image cells for the SRB condition (x-z view, the y-axis is perpendicular to the plane of the figure).

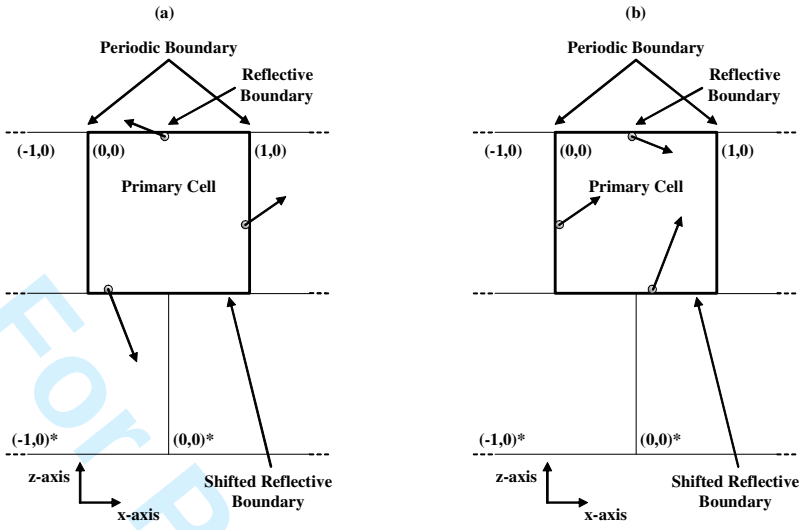

Figure 3: Re-insertion of particles in case of a SRB at the bottom wall, a simple reflective boundary at the top wall and a PB at the side walls: (a) before re-insertion, (b) after re-insertion.

The shifted reflective boundary

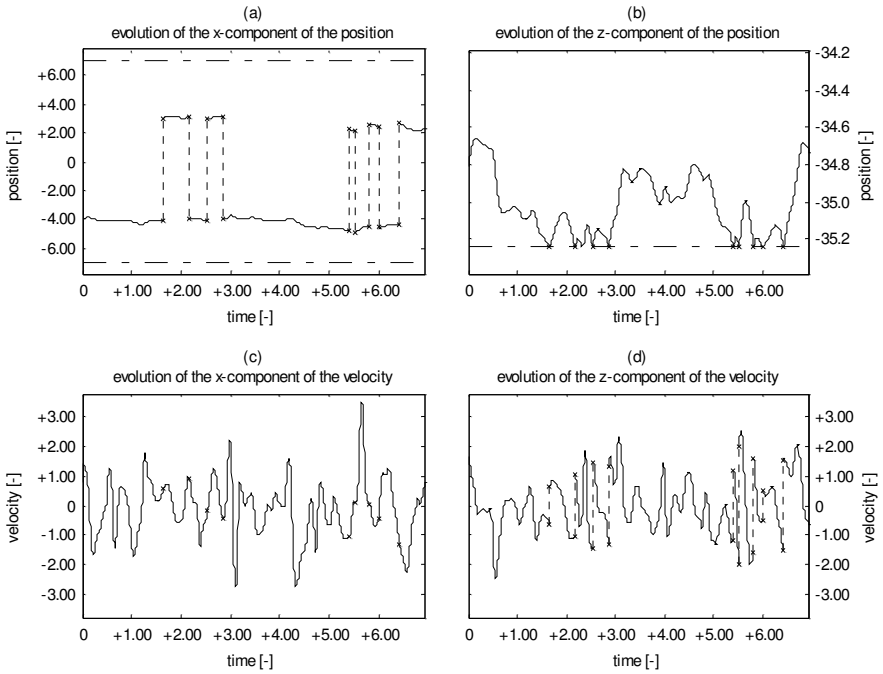

Figure 4: Evolution of the x-component (a) and z-component (b) of the position and of the x-component (c) and z-component (d) of the velocity as a function of time of a particle in the vicinity of the SRB for MD simulation A. All values are in reduced Lennard-Jones units.

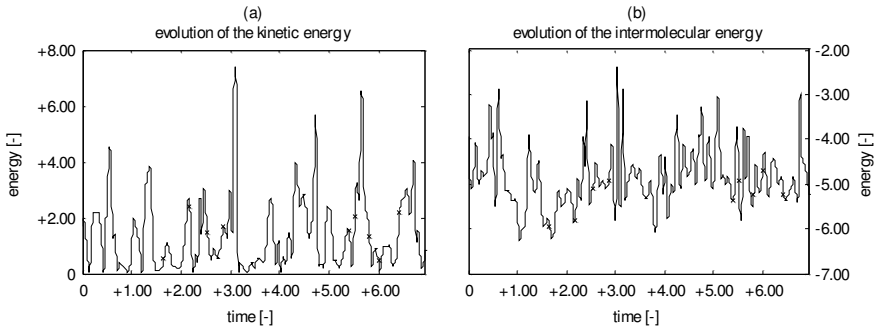

Figure 5: Evolution of the kinetic (a) and intermolecular (b) energy of a particle in the vicinity of the SRB condition for MD simulation A. All values are in reduced Lennard-Jones units.

The shifted reflective boundary

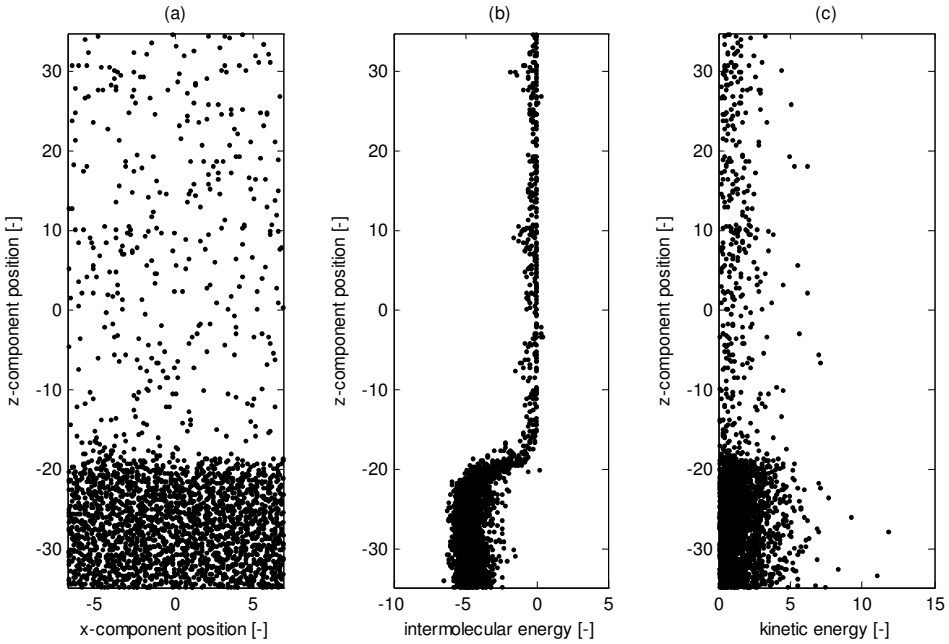

Figure 6: Results at the end of MD simulation B with a SRB at the bottom of the cell: (a) x-component of the position of the particles s a function of the z-position, (b) intermolecular energy per particle of the particles as a function of the z-position, (c) kinetic energy per particle of the particles as a function of the z-position. All values are in reduced Lennard-Jones units.

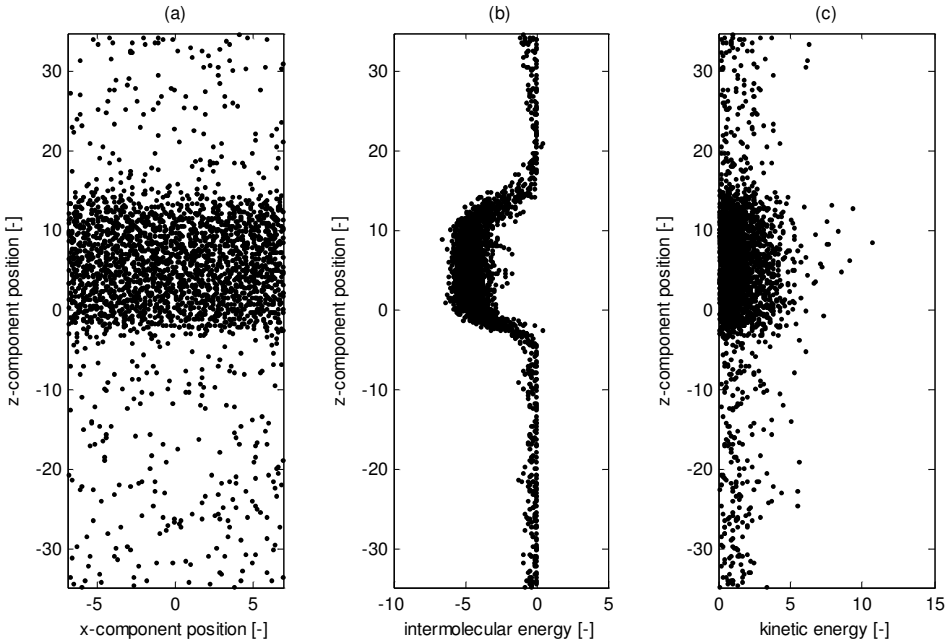

Figure 7: Results at the end of MD simulation C with a PB at the top and bottom of the cell: (a) x-component of the position of the particles s a function of the z-position, (b) intermolecular energy of the particles as a function of the z-position, (c) kinetic energy of the particles as a function of the z-position. All values are in reduced Lennard-Jones units.

The shifted reflective boundary

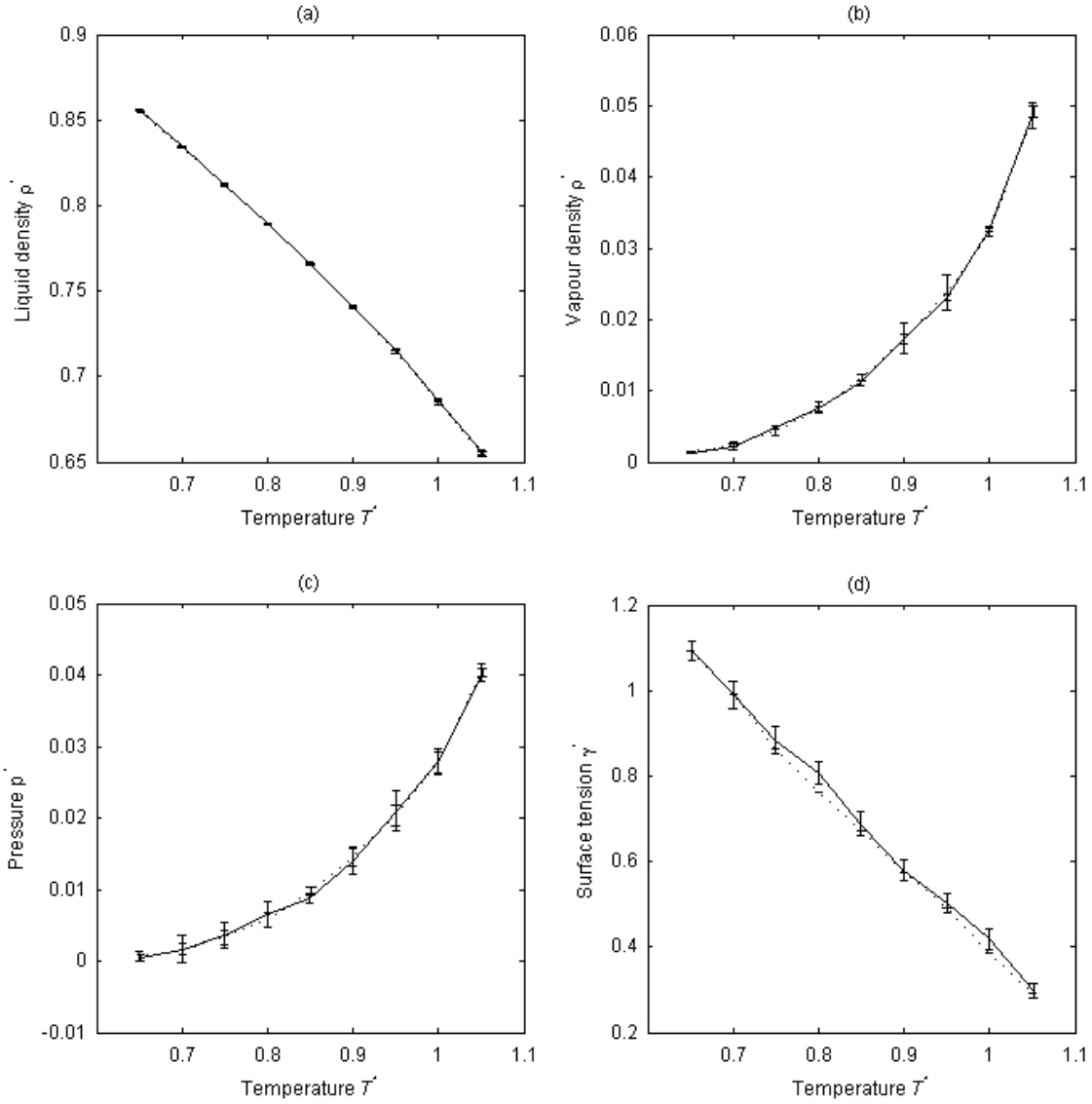

Figure 8 Evolution of the liquid density (a), the vapour density (b), the saturation pressure (c) and the surface tension (d) as a function of temperature of a two-phase system, for MD simulations D1-D9 with a SRB (solid line) and for MD simulations E1-E9 with PBs (dashed line). The error bars indicate the 95% confidence interval, see [12]. All values are in reduced Lennard-Jones units.

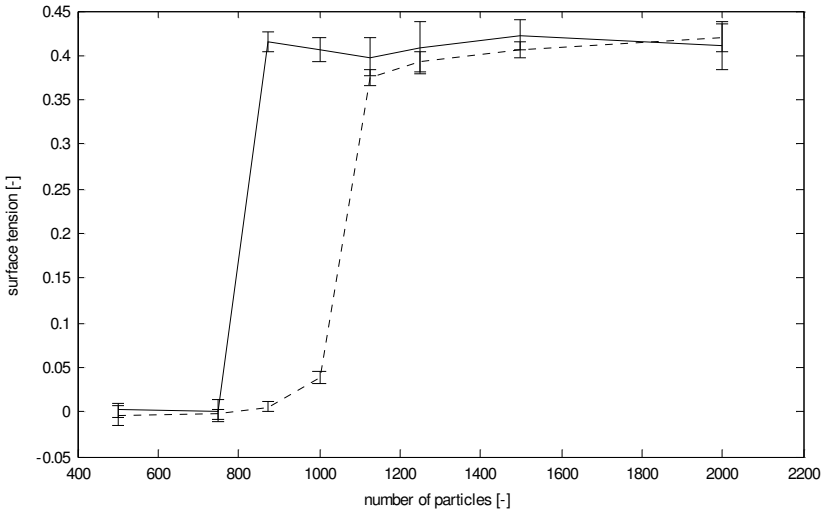

Figure 9: Evolution of the surface tension as a function of the number of particles for MD simulations F1-F8 with a SRB (solid line) and for MD simulations G1-G8 with PBs (dashed line). The error bars indicate the 95% confidence interval, see [12]. All values are in reduced Lennard-Jones units.

The shifted reflective boundary

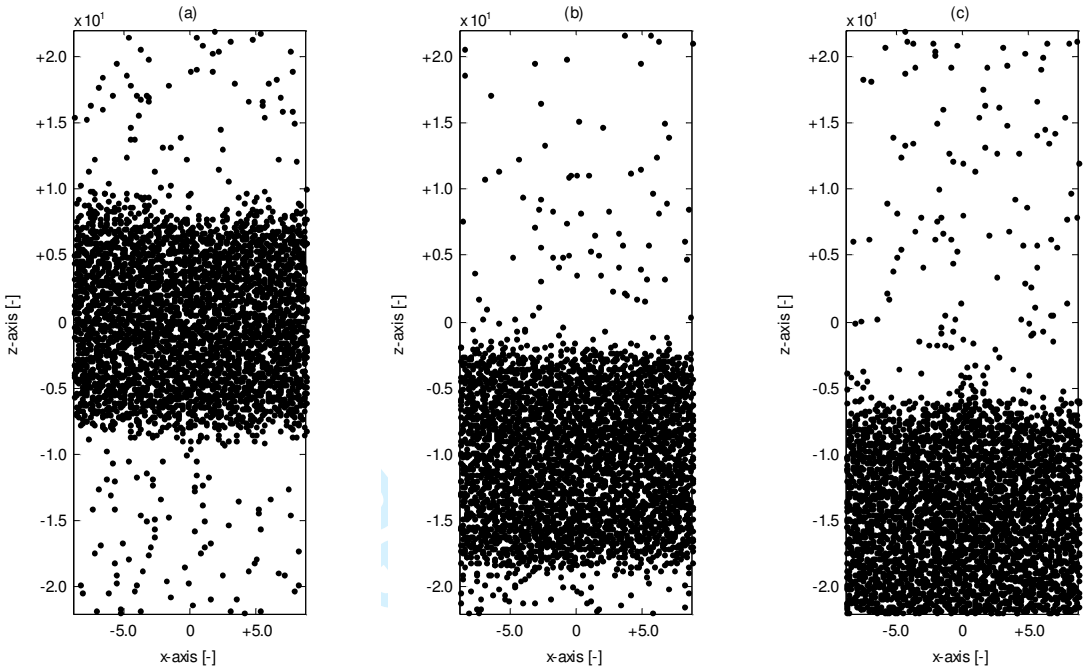

Figure 10: x-z-view of the initial state (a) at $t = 0$, of the intermediate state (b) at $t = 388$ and of the end state (c) at $t = 730$ of the particles in a two-phase system with a SRB condition at the bottom wall for MD simulation H. All values are in reduced Lennard-Jones units.

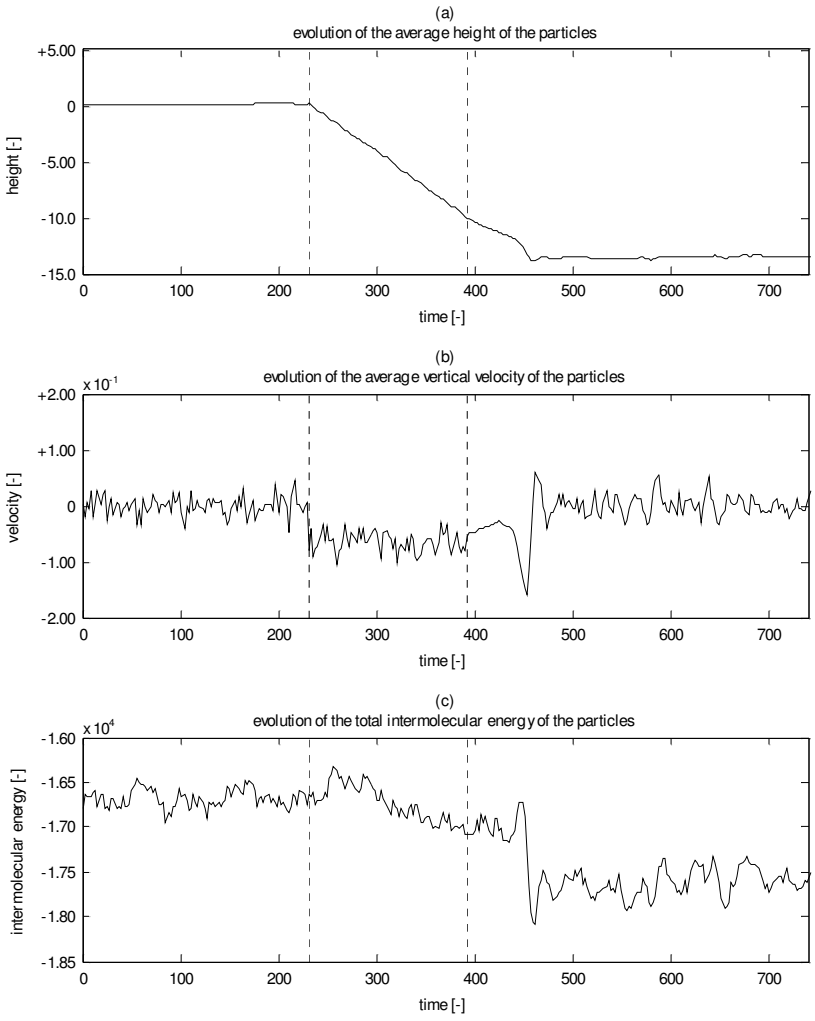

Figure 11: Evolution of the z-component of the position of the centre of mass (a), average vertical velocity (b) and total intermolecular energy (c) of the particles in a two-phase system with a SRB for MD simulation H. All values are in reduced Lennard-Jones units.

Submitted to Molecular Physics

The shifted reflective boundary for the study of two-phase systems with molecular dynamics simulations

Author Information

Geert Van den Branden

University of Leuven, K.U.Leuven,
Division of Applied Mechanics and Energy Conversion
Celestijnenlaan 300A, B-3001 Leuven, Belgium
Tel. +32 16 32 25 08
Fax +32 16 32 29 85
Email: geert.vandenbranden@mech.kuleuven.be

Martine Baelmans

University of Leuven, K.U.Leuven,
Division of Applied Mechanics and Energy Conversion
Celestijnenlaan 300A, B-3001 Leuven, Belgium
Tel. +32 16 32 25 11
Fax +32 16 32 29 85
Email: martine.baelmans@mech.kuleuven.be

William D'haeseleer

University of Leuven, K.U.Leuven,
Division of Applied Mechanics and Energy Conversion
Celestijnenlaan 300A, B-3001 Leuven, Belgium
Tel. +32 16 32 25 11
Fax +32 16 32 29 85
Email: william.dhaeseleer@mech.kuleuven.be

Submitted to Molecular Physics

The shifted reflective boundary for the study of two-phase systems with molecular dynamics simulations

G. VAN DEN BRANDEN, M. BAELMANS and W. D'HAESELEER*

University of Leuven, K.U.Leuven, Division of Applied Mechanics and Energy Conversion
Celestijnenlaan 300A, B-3001 Leuven, Belgium

When studying fluids with molecular dynamics simulations, periodic boundaries are usually used to model an infinite bulk fluid surrounding the primary cell. For homogeneous systems this is, as a rule, the most appropriate way. For inhomogeneous systems, e.g. systems with a fluid-vapour interface, periodic boundaries suffer some disadvantages. Therefore, an alternative for periodic boundaries, called shifted reflective boundary, is proposed for modelling such systems. From a computational point of view, this type of boundary is not more difficult to implement than periodic boundaries. It is shown that the shifted reflective boundary results in a stable spatial fluid-vapour configuration with one fluid-vapour interface, while retrieving the same numerical results for thermodynamic properties, e.g. the surface tension, as molecular dynamics simulations with periodic boundaries. Molecular dynamics simulations with shifted reflective boundaries also need fewer particles than corresponding simulations with periodic boundaries.

Keywords: Molecular Dynamics; Boundary Condition; Two-Phase Systems

* Corresponding author. Email: william.dhaeseleer@mech.kuleuven.be

1. Introduction

Molecular Dynamics (MD) simulation is a powerful and instructive numerical tool to study thermodynamic and kinetic processes in great detail, for i.a. the fluid-vapour interactions at the interface of a two-phase system. MD simulations are performed on a system of relatively small size in comparison with real thermodynamic systems (e.g. a system of 10^3 versus 10^{23} particles), thereby, nevertheless leading to statistically significant results. To model the world surrounding the MD system, different types of boundary conditions can be used (periodic, free, reflective), see [1]. For the study of single-phase systems, classical Periodic Boundaries (PB) are very appropriate. Unfortunately, PB conditions for two-phase vapour-liquid systems are not always appropriate to study the molecular processes at the interface. For that purpose, we would prefer a single flat interface remaining fixed in space. Therefore, we present a new type of boundary condition which is particularly adapted to study the two-phase vapour-liquid interface.

As a demonstration, Figure 1 (a) shows the results of a small MD simulation of Argon atoms in a system with a cubic cell with PB conditions. The forces between the Argon atoms are derived from a Lennard-Jones (LJ) potential. It is clear from this figure that the minimalisation of the free energy will result in a spherical-like interface. The position of the interface between the vapour and the liquid phase is not fixed since the droplet of liquid will wander throughout the system cell, and thereby possibly pass the PBs of the cell.

The spherical shape of the interface can be avoided by using a cell with a large aspect ratio. Minimalisation of the intermolecular energy by the system will result in a flat film of liquid surrounded by a vapour phase. Figure 1 (b) shows the result for a MD simulation of

Argon atoms in such a cell. This geometry of a double planar fluid-vapour interface has been used by among others [2-5] for their study of the interfacial properties of a LJ fluid. In principle, the liquid film will continue to randomly oscillate up and down the cell. Thermodynamic properties as pressure, temperature and surface tension can be calculated straightforward irrespective of these oscillations. For properties as the fluid and vapour densities, the presence of the oscillations can be sidestepped by monitoring the evolution of the centre of mass and continuously shifting the centre of mass of the cell back to a fixed position during the simulation. However, below we present a simpler and less intervening technique, whereby the fluid-vapour configuration is fixed through a specially adapted boundary condition the Shifted Reflective Boundary (SRB); which was developed to permit in a following stage the easy calculation of time correlation functions and pair-wise density functions at the interface.

The paper is organized as follows. In Section 2, we introduce the Shifted Reflective Boundary (SRB). Furthermore, in this section, the computational implications of the calculation of the intermolecular forces with SRBs are presented. In Section 3, we demonstrate some results of MD simulations using the SRBs: firstly, the individual behaviour of a particle in the vicinity of a SRB during a MD simulation; secondly, the collective behaviour of a two-phase system in a cell with a SRB compared to a corresponding MD simulation with PBs, thirdly, a quantitative comparison of two-phase MD calculations with SRBs and PBs for a range of temperature; fourthly the influence of the number of particles on the calculated surface tension in MD simulations with SRBs and PBs; finally, the stability of the fluid-vapour configuration in a MD simulation with a SRB.

2. Shifted reflective boundary condition

2.1. Rationale and principle

The purpose of the SRB is to model a system with one single fluid-vapour interface, whereby this interface, apart from naturally occurring variations, should remain fixed in space. This can be obtained when the boundary condition of one of the walls models the presence of an infinitely large unperturbed fluid phase. The fluid molecules in the cell will preferentially be present next to this boundary, since that position minimises their intermolecular energy. This way, the fluid phase stays attached to that boundary and, consequently, the vapour-liquid interface remains fixed in space.

The modelling of a liquid boundary condition, however, is not trivial. Indeed, a stationary attractive intermolecular force will not accurately predict the liquid behaviour. On the contrary, to model the liquid boundary condition, a dynamically varying force is needed to take into account the movement of molecules in a liquid. This movement of molecules is the most faithfully and the most easily modelled by using the liquid molecules already present in the primary cell during the MD simulations. This is the principle of the SRB condition presented in this paper.

2.2. Definition of the SRB

Like systems with PBs, a system with a SRB makes use of image cells but these image cells are defined in a different way. Figure 2 shows the primary cell of a system with a SRB at the bottom wall surrounded by its image cells. In the x- and y-direction the primary cell (0,0) is surrounded by classical periodic image cells (i,j). At the bottom, however, the primary cell is surrounded by shifted reflective image cells (i,j)*, these are specularly

reflected mirror images of the primary cell (and its periodic image cells) with the bottom wall serving as the plane of reflection, but whereby the image cell is simultaneously shifted in the x- and y-direction by a distance s_x and s_y respectively. (The shift s_y and the periodic repetition of cells in the y-direction are not visible in Figure 2.)

Defined as such, the SRB results, for particles i in the vicinity of the SRB, in intermolecular interactions with particles j^* which are image particles of particles j that are also situated in the vicinity of the SRB. Although the SRB condition has been defined to model a 'liquid boundary condition' to obtain a stable configuration of liquid and vapour, this boundary condition makes no a priori assumptions about the particle configuration and behaviour in the vicinity of the boundary, and, hence, it can also be used for other types of MD simulations, e.g. single-phase systems.

The boundary condition at the opposite boundary of a SRB, i.e. the top wall in Figure 2, can be a reflective boundary or another SRB, but not a PB, since this last boundary condition always has to be implemented in pairs. The boundary conditions in the x- and y-direction are restricted to PBs. For the purpose of clarity, a system with a simple reflective boundary condition at the top wall is used to illustrate the SRB in Figure 2. The shift (s_x,s_y) could in principle be freely chosen, but the most appropriate choice is a shift equal to half the dimensions of the primary cell in the x- and y-direction, $(s_x,s_y) = (\Delta x/2,\Delta y/2)$. From the definition of the SRB, it results that the x- and y-components of the velocities of a particle and it SRB image particle are equal, but that their z-component are opposite in sign.

2.3. Re-insertion of particles crossing a SRB

When, during a MD simulation, a particle happens to cross a SRB, it is re-inserted into the primary cell in the way shown in Figure 3. The z-component of the position of the particle remains unchanged, while the x- and y-component are increased by $\Delta x/2$ and $\Delta y/2$, respectively. Simultaneously, the z-component of the velocity of the particle is reversed while the x- and y-components remain unchanged; i.e., the moment a particle leaves the primary cell, it reappears with the position and velocity of its image particle. The particle loses or gains neither kinetic nor intermolecular energy in this procedure, as will be shown in Section 3.1. It is not necessary to perform the re-insertion transformation at the exact moment of boundary crossing. Particles can leave the primary cell during a calculation step, the moment a particle crosses the boundary, its image particle will enter the primary cell and particle and image particle temporarily switch roles.

However, as an alternative to the procedure described above, to determine the velocity of a re-inserted particle, the SRB permits to impose a wall temperature T, by randomly choosing the velocity of the re-inserted particle from a Maxwell-Boltzmann distribution at temperature T, see [6]. Since, with SRBs and in contrast to PBs, the opposite walls of a cell do not necessary have to be identical, the temperature at the SRB top wall and the SRB bottom wall can be different and a temperature gradient can be imposed.

2.4. Intermolecular force and cut-off radius

It is well known that, for systems with PBs, there will be intermolecular interactions between a particle i and its own image particles, if the intermolecular force has a long range with respect to the dimensions of the primary cell. In addition, there might be

intermolecular interactions between a particle *i* and several image particles of the same particle *j*. The same is true for systems with SRBs. Since the motion of a particle and the motion of its image particles are highly correlated, these kinds of interactions can hardly be considered to be realistic and have to be avoided in MD simulations.

In this section, we will determine the minimum dimensions necessary to achieve this, for a primary cell with a SRB as a function of the cut-off radius σ_c of the intermolecular forces, i.e. the distance between two molecules above which no intermolecular interaction occurs. For matters of comparison, we start with the relation between the minimum dimensions of the primary cell and the cut-off radius σ_c for a system with PBs.

For a primary cell with dimensions Δx, Δy and Δz, and with PBs, it is easy to show that no particle *i* interacts with periodic image particles *i*' of the particle *i* itself, if

$$\sigma_c < \min(\Delta x, \Delta y, \Delta z) . \tag{1}$$

In addition, each particle *i* only interacts with one single periodic image particle *j'* of particle *j* (or particle *j* itself), if, see [7],

$$\sigma_c < \min(\Delta x/2, \Delta y/2, \Delta z/2) . \tag{2}$$

For systems with a SRB at the bottom (or top) of a primary cell, the conditions imposed on the dimensions of the primary cell are more severe. No particle *i* interacts with a shifted reflective image particles *i** of the particle *i* itself, if

$$\sigma_c < \left((\Delta x/2)^2 + (\Delta y/2)^2\right)^{1/2} . \tag{3}$$

To impose that each particle *i* only interacts with the shifted reflective image particle *j** of particle *j* or one of the periodic image particles *j*' of particle *j* (including particle *j* itself), it is necessary that

The shifted reflective boundary

$$\sigma_c < \left((\Delta x/4)^2 + (\Delta y/4)^2\right)^{1/2}. \quad (4)$$

If there is a SRB at the top and bottom of the system, then there is the additional condition that

$$\sigma_c < \Delta z. \quad (5)$$

This last condition is only relevant for very wide and flat primary cells. For systems with a square base of the primary cell, i.e. $\Delta x = \Delta y$, comparison between the corresponding conditions for systems with PBs of equations (1) and (2), and the corresponding conditions for systems with SRBs of equations (3) and (4), show that the primary cell needs to be a factor $\sqrt{2}$ larger in the case of the SRBs to avoid the undesirable particle interactions. As such, this is a disadvantage of the use of a SRB. It has to be noted, however, that when neglecting the most stringent condition of equation (4), the undesirable intermolecular interactions only occurs for particles close to the SRB. No undesirable interactions can occur for particles at distances larger than the distance d_{max} from the SRB, with

$$d_{\max} = \left(\sigma_c^2 - (\Delta x/4)^2 - (\Delta y/4)^2\right)^{1/2}. \quad (6)$$

As such, only a very small fraction of the total number of particle interactions are to be considered unrealistic, all of which situated near boundary where the SRB has been applied. If equation (2) holds, in the worst case, only a fraction of less than 12% from all the intermolecular interactions between particles situated at a distance from the SRB smaller than $d_{\max}$ has to be considered as unrealistic.

2.5. Calculation of the intermolecular forces with shifted reflective boundaries

Due to the symmetry properties of the SRB condition with a shift of half a cell, the calculation of the intermolecular forces between particles and shifted reflected image

particles can be greatly simplified. When particle i interacts with an image particle j^* through an intermolecular force F_{ij*}, then there is also an intermolecular force F_{ji*} between a particle j due to an image particle i^* of equal magnitude. The orientation of both intermolecular forces however is slightly different,

$$F_{ij*} = F_{ji*}, \tag{7}$$

and

$$F_{ij*,x} = -F_{ji*,x} \;,\; F_{ij*,y} = -F_{ji*,y} \;,\; F_{ij*,z} = +F_{ji*,z} \,. \tag{8}$$

2.6. Comparison periodic boundaries and shifted reflective boundaries

In the previous sections, we have shown that SRBs with a shift of half a cell possess many symmetry properties similar to PBs. The result is that the MD simulations with SRBs require no extra computational effort compared to MD simulations with PBs. Table 1 gives an overview of the similarities and differences for a system with PBs and a system with a SRB at the bottom wall of the primary cell. In the following section, we will show that the SRB possesses all the properties we described above. It will also become clear that the SRB is a kind of hybrid boundary condition having features in common with both PBs and classical reflective boundaries.

2.7. The SRB and the finite size effect

It has been observed [8] that for small systems with PBs, the values of thermodynamic properties as pressure and surface tension are sensitive to cell geometry and size. For increasing cell dimensions, the value of the observed variables converges periodically or monotonically towards the thermodynamic value. Using large cells (with more particles) can resolve this problem, but at the cost of larger computational time. Since SRBs are periodic in nature in the x and y-direction, it can be expected that they suffer from the

same finite size effect. However, as will be shown in Section 3.4, for a cell of fixed size, a system with SRBs needs fewer particles to obtain a stable fluid-vapour interface than a system with PBs. Hence, for a fixed number of particles, larger cells can be used.

3. Results of MD simulations with a shifted reflective boundary

3.1. Behaviour of a particle in the vicinity of a shifted reflective boundary

In Section 2, we defined the SRB. In this section, we illustrate the effect of the SRB on the behaviour of a single particle in the vicinity of a SRB during MD simulation A. The parameters and results of this and all subsequent MD simulations are conventionally rendered dimensionless using reduced Lennard-Jones units, see among others [5], length $z^* = z/\sigma$, energy $e^* = e/\varepsilon$, time $t^* = t\sqrt{\varepsilon/m}/\sigma$, temperature $T^* = k_B T/\varepsilon$, pressure $p^* = p\sigma^3/\varepsilon$, surface tension $\gamma^* = \gamma\sigma^2/\varepsilon$, velocity $v^* = v\sqrt{m/\varepsilon}$. The system consists of 3685 LJ particles in a cell of dimensions 14.1 × 14.1 × 70.5. The boundaries the in x- and y-directions are PBs. In the z-direction, at the bottom wall (z = -34.78), a SRB is implemented, whereas at the top wall (z = +34.78) a reflective boundary is present. The temperature of the system is 0.98 using Andersen's thermostat [8]. The cut-off ratio used for this and all subsequent calculations is 3.45 σ. Table 2 gives an overview of the principal parameters of the MD simulations.

Figure 4 shows the evolution of the x- and z-components of the position and the velocity of a single particle during MD simulation A. The y-component is not depicted but the evolution of this component is similar to that of the x-component. Although the duration of this MD simulation was much longer, the time span of the plotted results is limited to 6.84 in order not to overload the figure. In Figure 4 (a) and (b), the boundaries of the primary

cell are indicated with a dash-dot line. The particle crosses the SRB at the bottom of the cell (z = -34.78) on several occasions. The different instances of boundary crossings are marked with the symbol ×.

Figure 4 (a) and Figure 4 (c) show the evolution of the x-components of the position and the velocity of the particle, respectively. Each boundary crossing involves a discontinuity in the x-component of the position of the particle, whereby the particle is shifted by half a cell width, see Figure 4 (a). The x-component of the velocity, however, remains unchanged when crossing a SRB, see Figure 4 (c).

The evolution of the z-components of the position and the velocity is completely different, see Figure 4 (b) and Figure 4 (d), respectively. There are no discontinuities present in the z-component of the position of the particle, see Figure 4 (b), while the sign of the z-component of the velocity is reversed every time the particle crosses the SRB, see Figure 4 (d). Notwithstanding the seemingly discontinuous behaviour of the particle when crossing a SRB, the particle experiences a smooth transition, as was mentioned in Section 2.2. This can be seen in Figure 5, where the evolution of the kinetic and intermolecular energy of the same particle is depicted, again with the boundary crossings marked with the symbol ×. The evolution of the kinetic and the intermolecular energy are both continuous, meaning that no energy is lost or gained when crossing the SRB.

For clarity, during this MD simulation the particle is shifted and the velocity is reversed at exactly the moment of the boundary crossing. As previously stated, this is not compulsory.

3.2. Molecular dynamics simulation of a system of LJ particles

In this section, we will present a typical result of a two-phase MD simulation with a SRB condition and compare it with the results of a two-phase MD simulation of a system with PBs. For MD simulation B, with the SRB, the set-up is the same as MD simulation A of the previous section. For MD simulation C, PBs are implemented in the z-direction instead of SRBs, see also Table 2.

Figure 6 (a) shows the position of the particles at the end of MD simulation B. As we envisaged in Section 2, most particles are present in the liquid phase at the bottom of the cell, due to the SRB situated at $z = -\Delta z/2$.

Figure 7 (a) shows the position of the particles at the end of MD simulation C. The result is typical for a two-phase system in a cell with PBs. Although the fluid phase was initially perfectly centred, due to the fluctuations during the MD simulations, it has slowly moved upwards.

Very interesting is the comparison of the vertical distribution of the particles as a function of their kinetic and intermolecular energy for MD simulation B with a SRB, see Figure 6 (b) and (c), and the same distribution for MD simulation C for PBs, see Figure 7 (b) and (c). The two different phases are very distinctively recognisable in both figures, firstly, due to the fact that the fluid phase has a much larger density than the vapour phase and, secondly, because particles in the fluid phase, on average, have a much larger intermolecular energy (in the sense of a larger absolute value, although the attractive intermolecular forces are conventionally considered as being negative). Figure 6 also shows that the presence of a SRB does not change the properties of the fluid phase in its

vicinity. The fluid phase behaves as if it is bounded at the bottom of the primary cell by an infinite bulk fluid.

The number of particles in both MD simulations being identical, it is clear that the number of particles at the interface between vapour and fluid is twice as large in the MD simulation with PBs (Figure 7) compared to the MD simulation with a SRB (Figure 6) and that, consequently, the number of bulk fluid particles is larger in MD simulations with a SRB. If the number of particles in the MD simulation is too small, no bulk fluid phase will develop, and the results will not be representative for real fluid-vapour systems. As a consequence, MD simulations with a SRB require a lower number of particles than corresponding MD simulations with PBs. This will be demonstrated in detail in the next section.

3.3. Comparison of two-phase systems with SRBs and systems with PBs

In this Section, the results of MD simulations of two-phase systems with SRBs and PBS are compared for temperatures T^* ranging from 0.65 to 1.05, see Table 2 for the principal parameters of the different MD simulations. For the MD simulations with PBs (MD simulations E1-E9), after each time step, the centre of mass of the particles was reshifted to the geometrical centre of the cell. For systems with SRBs (MD simulations D1-D9), no measures had to be taken to keep the fluid phase fixed at the bottom of the cell. Figure 8 shows the results of the MD calculations for both types of boundary conditions as a function of temperature. Figure 8 (a) en (b) show the fluid and vapour densities of the two-phase state, respectively. Figure 8 (c) shows the corresponding saturation pressure and Figure 8 (d) the surface tension. The surface tension is classically calculated as the

difference of the normal and the transverse component of the pressure, see among others [10]. The results for the MD calculation with SRBs (solid line) correspond well with the results for the MD calculation with PBs (dashed line) over the whole range of temperatures. The presence of the SRBs instead of the classical PBs does not change the thermodynamic properties of the system, as was required.

3.4. Effect of the number of particles

In Section 2, it was stated that a SRB has the advantage that it will provide statistically significant results even with fewer particles in the MD simulation than a corresponding simulation with PB conditions and this due to the fact that only one interface is present. In this section, the evolution of the surface tension for different MD simulations is presented as a function of the number of particles N. The basic set-up is identical as in the previous sections, with the sole exception of the total number of particles, the dimensions of the cell are constant for all simulations, irrespective of the number of particles. For the MD simulations F1 through F8, the boundary in the z-direction at the bottom of the primary cell (z = -34.78) is a SRB, the boundary at the top (z = -34.78) is a reflective boundary. For MD simulation G1 through G8, the boundaries in the z-direction are PBs. The number of particles N in the MD simulations varies for MD simulations F1 through F8 (and correspondingly G1 through G8), and equals 500, 750, 875, 1000, 1125, 1250, 1500 and 2000, respectively, see Table 2 for more details on MD simulations F and G . The initial configuration of the particles was constructed in such a way that a liquid and vapour phase were present. The particle distribution for the liquid and vapour phase was taken from a previous MD simulation at the same temperature. Figure 9 shows the surface tension as a

function of the number of particles *N*. For large number of particles *N*, both systems with SRBs and PBS obtain the same values for the surface tension, corresponding with the results given by [11]. On the other hand, for systems with small values of *N*, and notwithstanding the careful preparation of the initial configuration, the liquid phase breaks up during the MD calculation, resulting in a homogeneous phase and, consequently, zero surface tension. However, it is clear, from this figure, that fewer particles are required for an accurate result with a SRB than in case of a system with PBs.

3.5. Stability of a system with a shifted reflective boundary

When a SRB is present at one of the boundaries of a primary cell, the fluid phase of a two-phase fluid-vapour system will reside preferentially at the SRB. To illustrate this, the evolution of the spatial configuration a two-phase fluid-vapour system is calculated for a system with a SRB at the bottom of the primary cell (MD simulation H). The initial condition of the system is a fluid phase centred in the middle of the cell surrounded on top and bottom by a vapour phase in equilibrium with this fluid phase. This initial condition was the result of a previous MD simulation with a PB. Equilibrium between the vapour and fluid phase was attained, while actively fixing the position of the fluid droplet by continuously resetting the centre of mass of the system to the middle of the cell. The initial state is shown in Figure 10 (a). The system consists of 3687 particles in a primary cell of dimensions $17.4 \times 17.4 \times 43.48$. The boundary conditions in the x- and y-directions are PB conditions. The temperature of the system is 0.87 using Anderson's thermostat.

During MD simulation H, the fluid phase was not centred. Due to fluctuations caused by the Andersen's thermostat the system is expected to wander up and down the primary cell,

eventually reaching the SRB at the bottom of the cell. The time it would take to reach the bottom of the primary cell, solely as a result of statistical fluctuations, would be, according to MD measures, astronomical. Since we are mainly interested in the fluid phase interacting with the SRB, we give the particles, between a time $t = 228$ and $t = 388$, through the thermalisation process, on average a little downwards velocity of 0.64. This push does not incriminate the results of this MD simulation, since the fluid phase would eventually have reached the SRB at the bottom of the cell at some point in time, though probably with a lower mean velocity. At time $t = 388$, the fluid droplet approaches the bottom of the cell, see Figure 10 (b), and no downwards push is further on applied. When the MD simulation would have employed a simple reflective boundary, the fluid phase would have bounced back upwards. With a PB, the fluid phase would have continued to go downwards and would have reappeared at the top of the cell. With the SRB, the fluid phase stays attached at the bottom of the cell, as can be seen from Figure 10 (c).

Figure 11 depicts the evolution of the vertical position of the centre of mass, the average vertical velocity and the total intermolecular energy of the system as a function of time. In the first stage of the simulation (from $t = 0$ till $t = 228$), without the downward push, the vertical velocity of the system fluctuates around zero and, hence, the vertical position of the centre of mass does not change significantly. The intermolecular energy, apart from some naturally occurring fluctuations, remains constant.

During the second stage of the simulation (from $t = 228$ till $t = 388$), with the downward push, the z-component of the average velocity of the system fluctuates, as expected, around the value -0.64. Accordingly, the z-component of the position of the centre of mass of the system decreases, and the fluid-phase, in which most particles reside, is moving

downwards. After a while, the intermolecular energy of the system starts to decrease, since fluid particles begin to interact with SRB image particles and the LJ potential at long intermolecular distances is attractive.

During the third stage of the simulation (from $t = 388$ till $t = 730$), again without downward push, the fluid phase first starts to slow down in its downward movement. This is due to the reflective character of the SRB. Particles crossing the SRB are re-inserted into the primary cell with an upwards velocity, thereby decreasing the overall downward velocity of the system. However, when the fluid phase further approaches the SRB, the attractive intermolecular forces of SRB image particles on the fluid phase gain the upper hand and accelerate the fluid phase downwards to the SRB. When the fluid phase crosses the SRB, many particles are re-inserted with an upwards velocity, and the downward movement is abruptly halted, see Figure 11 (b). From this moment one the average vertical velocity fluctuates around a value of zero and the vertical position of the centre of mass fluctuates around its equilibrium position, with the fluid phase attached to the SRB, see Figure 11 (a). At the start of the third stage, when the fluid-phase is still moving downwards, the intermolecular energy continues to decrease, see Figure 11 (c). However, the moment the fluid-phase reaches the SRB with a large downward velocity, the particles and image particles approach each other at relatively short intermolecular distances, at which the LJ intermolecular forces become repulsive, resulting in an increase in intermolecular energy and a further halt to the downwards movement. As soon as this short transitional phase ends, the particles and image particles resettle and, through their mutual attractive interactions, the intermolecular energy of the system strongly decreases.

The shifted reflective boundary

The low intermolecular energy signifies that more particles are *bulk* liquid particles with a lower intermolecular energy, when the fluid phase resides at the bottom of the cell, and consequently in the vicinity of the SRB, than when the fluid phase resides away from the SRB. In fact, when the fluid phase is situated at the bottom of the cell, there is only one single fluid-vapour interface left of the two interfaces present at the start of the simulation. The particles at the bottom interface have all been transformed into bulk fluid particles, hence decreasing the intermolecular energy.

Figure 11 shows that the randomly occurring fluctuations of the intermolecular energy are much smaller than the difference in intermolecular energy between a fluid phase which is detached from a SRB and a fluid phase which is attached to a SRB. This means that the probability that the fluid phase detaches from the SRB due to statistical thermal fluctuations is very small and that the system will preferentially resides in the part of phase-space with the fluid phase attached to the SRB.

The stability of the final configuration, as shown in Figure 10, can be further quantified when looking at the difference in average total intermolecular energy between the two-phase system with two interfaces in the first stage of the simulation (from $t = 0$ to 388) and the two-phase system with one interface in the final stage of the simulation (from $t = 502$ to 730). The average of the total intermolecular energy of the system with two interfaces is -16 685±42, the average of the total intermolecular energy of the system with one interface is -17 606±36, a difference of 922±55. This value has to be compared with the variance around the total intermolecular energy of the system with one interface, which equals 139. If we assume that the accessible states are Gaussian distributed around the most probable

state, see [13], then the system has only a probability of approximately one in 6×10^{10} to reside in a state with a detached liquid phase.

This has two consequences. Firstly, for a system with a SRB, the initial condition of a MD simulation is very important, more than with PBs, in order to keep the simulation within realistic computational times. Indeed, although a fluid phase at the centre or at the top of the primary cell is not excluded, the fluid phase at the bottom of the cell is much more probable and therefore much more representative of all possible systems in phase space. Secondly, since the chance of detaching from the SRB is very small, there is no need to actively monitor and fix the position of the fluid phase in the primary cell, as is usually done during MD simulations employing PBs. With a SRB, the fluid phase stays fixed in a very natural way. The height of the fluid-vapour interface, though, can vary a bit through statistical fluctuations, as it would be expected. This feature was one of the main reasons for the development of the SRB.

4. Conclusions

In this paper, we have presented a special type of boundary condition: the shifted reflective boundary condition for molecular dynamics simulations of systems with a vapour-liquid interface. Notwithstanding the seemingly artificial character of this boundary condition, this boundary condition is clearly capable of calculating the properties of a two-phase system. Compared to PBs, the shifted reflective boundary has the advantage that fewer particles are situated at the fluid-vapour interface, thereby reducing the minimum number of particles needed in a two-phase simulation. Secondly, since in a system with a shifted

reflective boundary the fluid phase stays attached at the shifted reflective boundary, the detailed study of the interface properties and processes can be greatly facilitated.

References

[1] Daan Frenkel and Berend Smit, Understanding Molecular Simulation, Academic Press, San Diego (2002).

[2] M.J.P. Nijmeijer, A.F. Bakker, C. Bruin, J. Chem. Phys., **89**, 3789 (1988).

[3] Andrij Trokhymchuk, José Alejandre, J. Chem. Phys., **111**, 8510 (1999).

[4] Daniel Duque, Lourdes F. Vega, J. Chem. Phys. **121**, 8611 (2004).

[5] Jadran Vrabec, Gaurav Kular Kedia, Guido Fuchs, Hans Hasse, Mol. Physics., **104**, 1509 (2006).

[6] Alexander Tenenbaum, Giovanni Ciccotti, Renato Gallico, Phys. Rev. A., **25**, 2778 (1982).

[7] Doros N. Theodorou and Ulrich W. Suter, J. Chem. Phys. **82**, 955 (1985)

[8] Minerva González-Melchor, Pedro Orea, Jorge López-Lemus, Fernando Bresem, José Alejandre, J. Chem. Phys. 122,094503 (2005)

[9] Andersen, H.C., J. Chem. Phys., **72**, 2384 (1980)

[10] John G. Kirkwood, Frank. P. Buff, J. Chem. Phys., **17**, 338 (1949)

[11] V.G. Baidakov, G.G. Chernykh, S.P. Protsenko, Chem. Phys. Lett., **321**, 315 (2000).

[12] J.M. Haile, Molecular Dynamics Simulation, John Wiley & Sons, New York (1992).

[13] F. Reif, Fundamentals of Statistical and Thermal Physics, McGraw-Hill, New York (1965).

Table 1: Comparison of Periodic and Shifted Reflective Boundary Condition

	Periodic Boundary	Shifted Reflective Boundary
transformation rule position image particle	$x \rightarrow x + m\,\Delta x$ $y \rightarrow y + n\,\Delta y$ $z \rightarrow z + p\,\Delta z$ m, n, p any integer number	$x \rightarrow x + \Delta x/2 + m\,\Delta x$ $y \rightarrow y + \Delta y/2 + n\,\Delta y$ $z \rightarrow - \Delta z - z$ m, n any integer number
transformation rule velocity image particle	$v_x \rightarrow v_x$ $v_y \rightarrow v_y$ $v_z \rightarrow v_z$	$v_x \rightarrow v_x$ $v_y \rightarrow v_y$ $v_z \rightarrow - v_z$
relationship between the intermolecular force F_{ij*} on particle i due to nearest image particle of j and the intermolecular force F_{ji*} on particle j due to nearest image particle of i	$F_{x,ij*} = - F_{x,ji*}$ $F_{y,ij*} = - F_{y,ji*}$ $F_{z,ij*} = - F_{z,ji*}$	$F_{x,ij*} = - F_{x,ji*}$ $F_{y,ij*} = - F_{y,ji*}$ $F_{z,ij*} = + F_{z,ji*}$

The shifted reflective boundary

Table 2 Overview of the principal parameters of the MD simulations. All values are in reduced Lennard-Jones units. The boundary condition indicated is the boundary condition in the z-direction. The boundary conditions in the x- and y-direction are always PBs.

Name	Dimensions $\Delta x^* \times \Delta y^* \times \Delta z^*$	Boundary condition	Temperature	Number of Particles
A	14.1 × 14.1 × 70.5	SRB	0.98	3685
B	14.1 × 14.1 × 70.5	SRB	0.98	3685
C	14.1 × 14.1 × 70.5	PB	0.98	3685
D1-D9	17.4 × 17.4 × 43.48	SRB	0.65, 0.7, 0,75, 0.8, 0.85, 0.9, 0.95, 1.0, 1.05	3685
E1-E9	17.4 × 17.4 × 43.48	PB	0.65, 0.7, 0,75, 0.8, 0.85, 0.9, 0.95, 1.0, 1.05	3685
F1-F8	14.1 × 14.1 × 70.5	SRB	0.98	500, 750, 875, 1000, 1125, 1250, 1500, 2000
G1-G8	14.1 × 14.1 × 70.5	PB	0.98	500, 750, 875, 1000, 1125, 1250, 1500, 2000
H	17.4 × 17.4 × 43.48	SRB	0.87	3687

List of Figure Captions

Figure 1: x-z –projection of Argon atoms particles in a MD simulation in a cubic cell with PB conditions (a) and x-z –projection of Argon atoms in a MD simulation in a cuboid cell with PB conditions (b).

Figure 2: Lay-out of the primary cell and the image cells for the SRB condition (x-z view, the y-axis is perpendicular to the plane of the figure).

Figure 3: Re-insertion of particles in case of a SRB at the bottom wall, a simple reflective boundary at the top wall and a PB at the side walls: (a) before re-insertion, (b) after re-insertion.

Figure 4: Evolution of the x-component (a) and z-component (b) of the position and of the x-component (c) and z-component (d) of the velocity as a function of time of a particle in the vicinity of the SRB for MD simulation A.

Figure 5: Evolution of the kinetic (a) and intermolecular (b) energy of a particle in the vicinity of the SRB condition for MD simulation A.

Figure 6: Results at the end of MD simulation B with a SRB at the bottom of the cell: (a) x-component of the position of the particles s a function of the z-position, (b) intermolecular energy of the particles as a function of the z-position, (c) kinetic energy of the particles as a function of the z-position.

Figure 7: Results at the end of MD simulation C with a PB at the top and bottom of the cell: (a) x-component of the position of the particles s a function of the z-position, (b)

intermolecular energy of the particles as a function of the z-position, (c) kinetic energy of the particles as a function of the z-position.

Figure 8: Evolution of the liquid density (a), the vapour density (b), the saturation pressure (c) and the surface tension (d) as a function of temperature of a two-phase system, for MD simulations D1-D9 with a SRB (solid line) and for MD simulations E1-E9 with PBs (dashed line). The error bars indicate the 95% confidence interval, see [12]. All values are in reduced Lennard-Jones units.

Figure 9: Evolution of the surface tension as a function of the number of particles for MD simulations F1-F8 with a SRB (solid line) and for MD simulations G1-G8 with PBs (dashed line). The error bars indicate the 95% confidence interval, see [11].

Figure 10: x-z-view of the initial state (a) at t = 0, of the intermediate state (b) at t = 388 and of the end state (c) at t = 730 of the particles in a two-phase system with a SRB condition at the bottom wall for MD simulation H.

Figure 11: Evolution of the z-component of the position of the centre of mass (a), average vertical velocity (b) and total intermolecular energy (c) of the particles in a two-phase system with a SRB for MD simulation H.

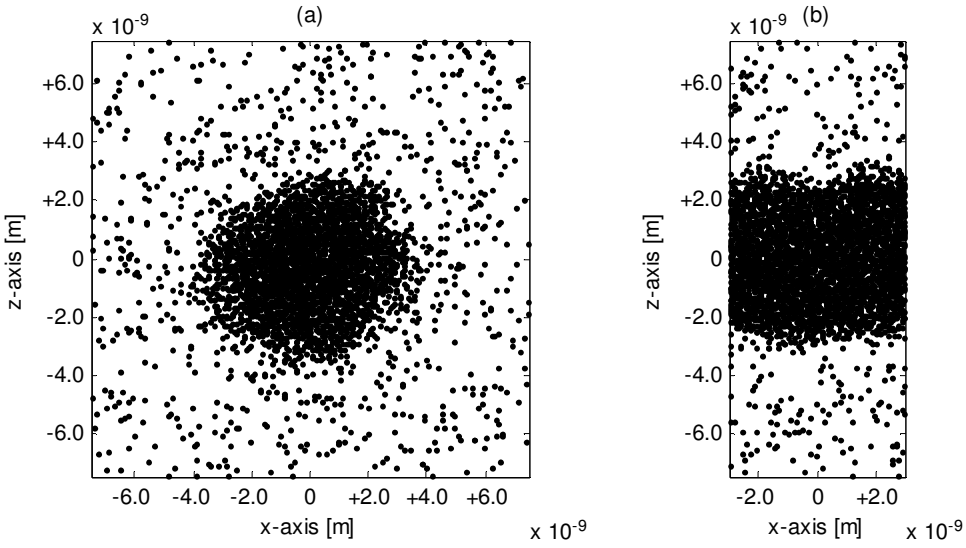

Figure 1: x-z –projection of Argon atoms particles in a MD simulation in a cubic cell with PB conditions (a) and x-z –projection of Argon atoms in a MD simulation in a cuboid cell with PB conditions (b).

The shifted reflective boundary

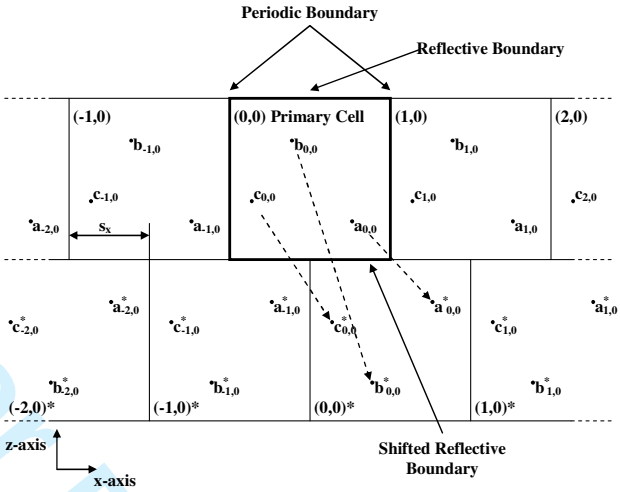

Figure 2: Lay-out of the primary cell and the image cells for the SRB condition (x-z view, the y-axis is perpendicular to the plane of the figure).

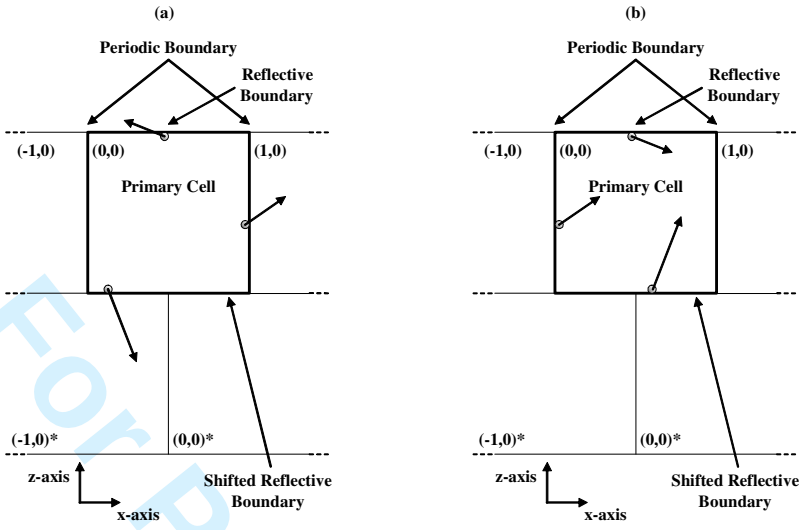

Figure 3: Re-insertion of particles in case of a SRB at the bottom wall, a simple reflective boundary at the top wall and a PB at the side walls: (a) before re-insertion, (b) after re-insertion.

The shifted reflective boundary

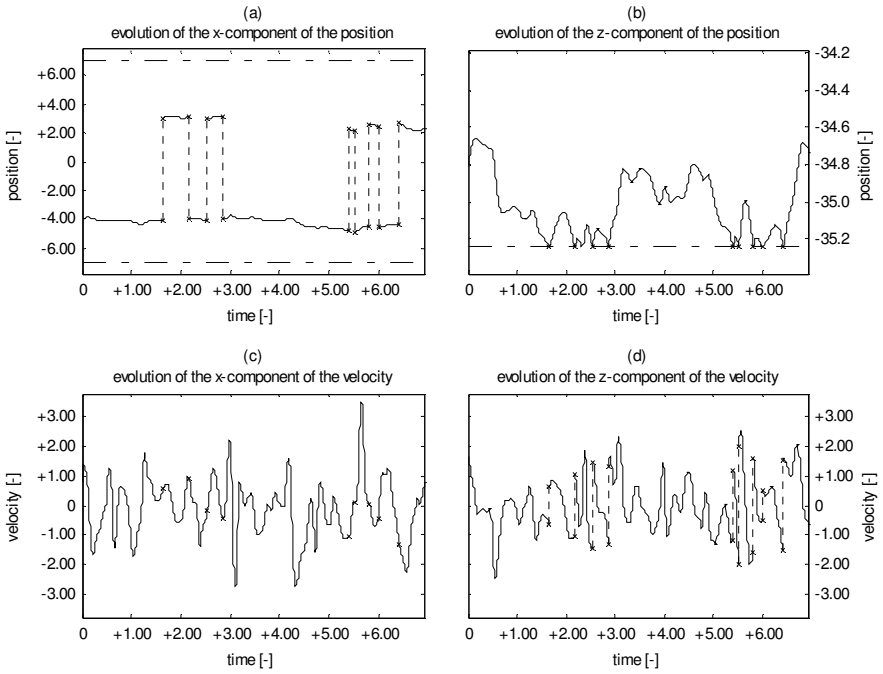

Figure 4: Evolution of the x-component (a) and z-component (b) of the position and of the x-component (c) and z-component (d) of the velocity as a function of time of a particle in the vicinity of the SRB for MD simulation A. All values are in reduced Lennard-Jones units.

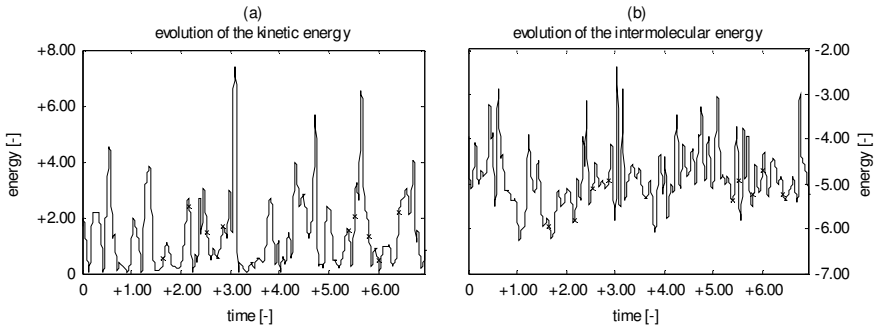

Figure 5: Evolution of the kinetic (a) and intermolecular (b) energy of a particle in the vicinity of the SRB condition for MD simulation A. All values are in reduced Lennard-Jones units.

The shifted reflective boundary

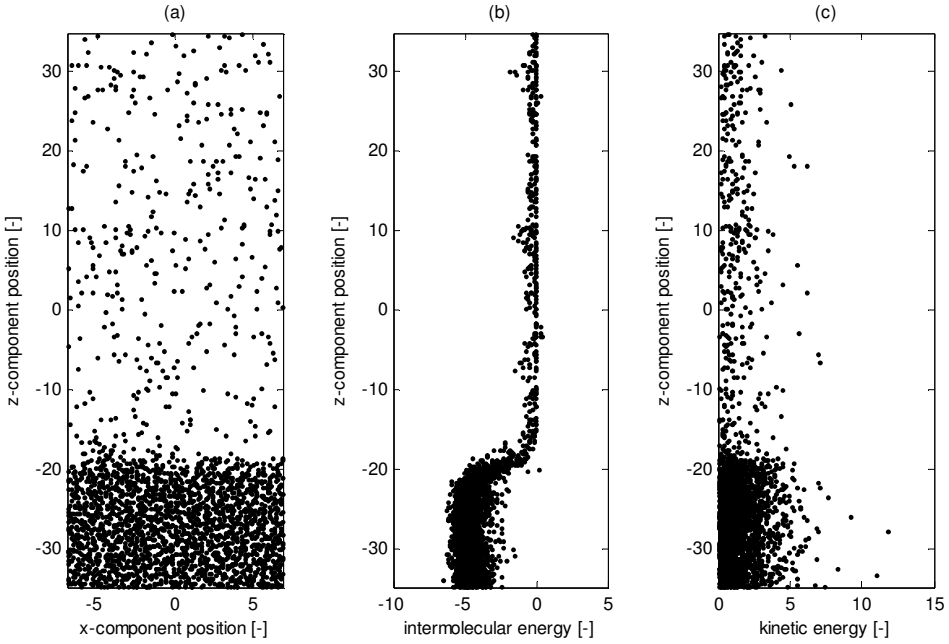

Figure 6: Results at the end of MD simulation B with a SRB at the bottom of the cell: (a) x-component of the position of the particles s a function of the z-position, (b) intermolecular energy per particle of the particles as a function of the z-position, (c) kinetic energy per particle of the particles as a function of the z-position. All values are in reduced Lennard-Jones units.

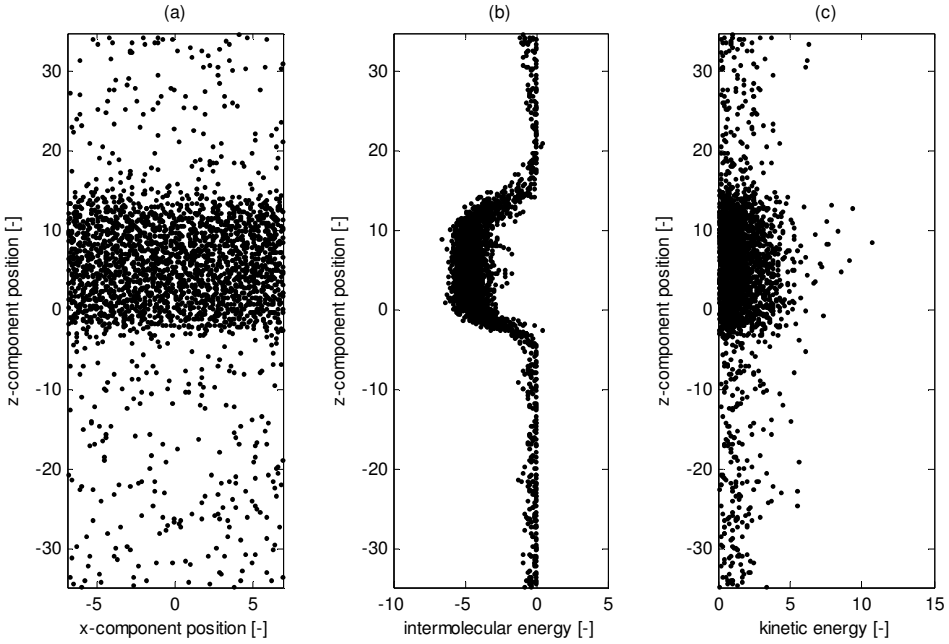

Figure 7: Results at the end of MD simulation C with a PB at the top and bottom of the cell: (a) x-component of the position of the particles s a function of the z-position, (b) intermolecular energy of the particles as a function of the z-position, (c) kinetic energy of the particles as a function of the z-position. All values are in reduced Lennard-Jones units.

The shifted reflective boundary

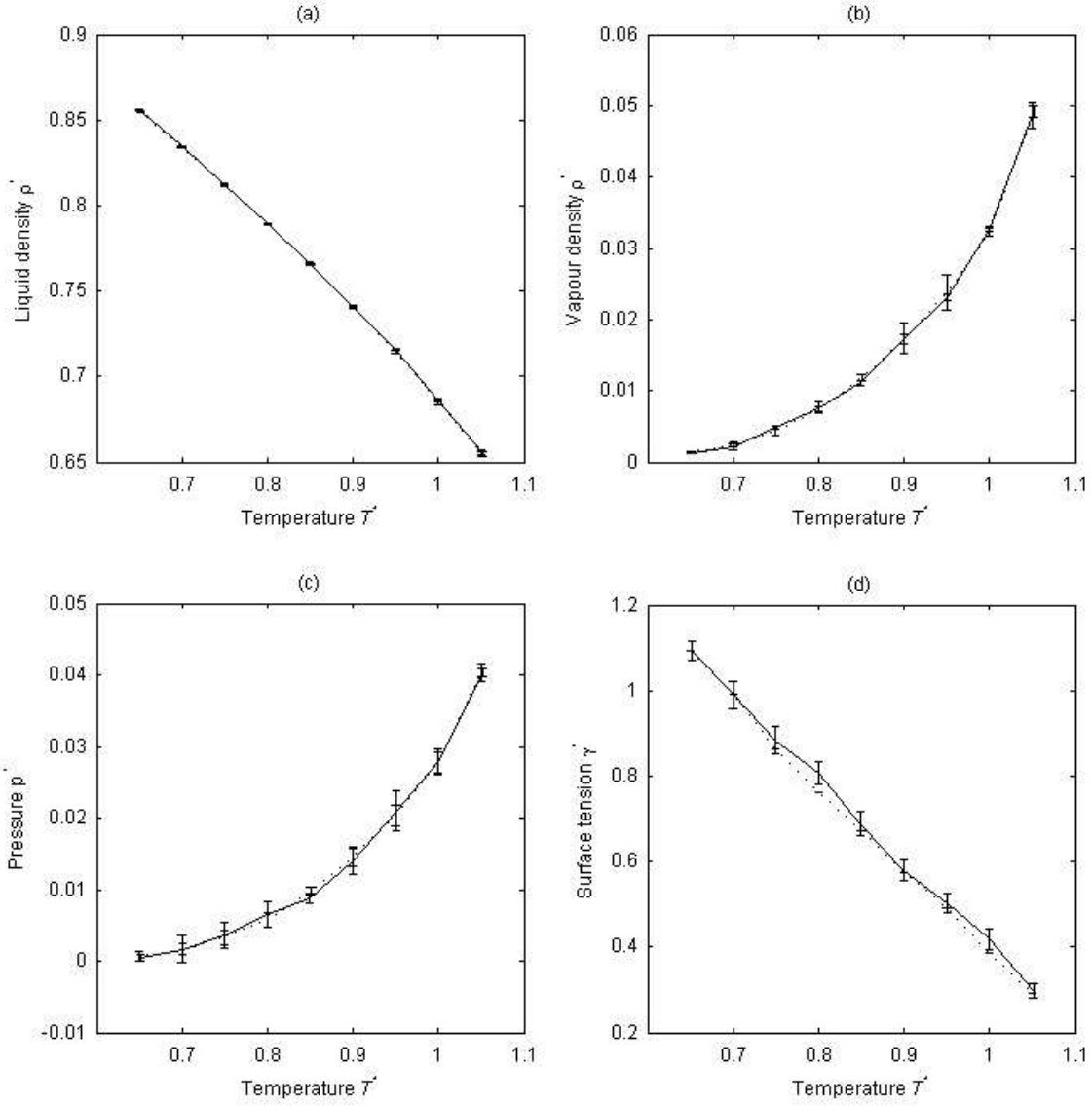

Figure 8 Evolution of the liquid density (a), the vapour density (b), the saturation pressure (c) and the surface tension (d) as a function of temperature of a two-phase system, for MD simulations D1-D9 with a SRB (solid line) and for MD simulations E1-E9 with PBs (dashed line). The error bars indicate the 95% confidence interval, see [12]. All values are in reduced Lennard-Jones units.

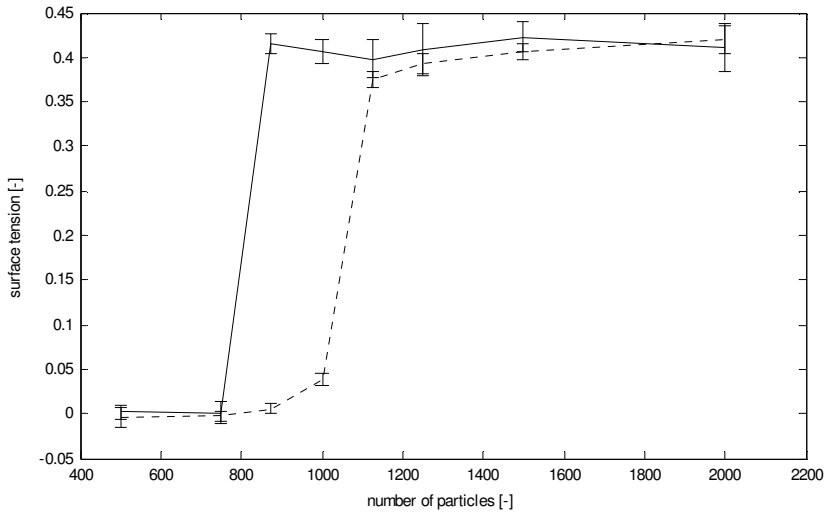

Figure 9: Evolution of the surface tension as a function of the number of particles for MD simulations F1-F8 with a SRB (solid line) and for MD simulations G1-G8 with PBs (dashed line). The error bars indicate the 95% confidence interval, see [12]. All values are in reduced Lennard-Jones units.

The shifted reflective boundary

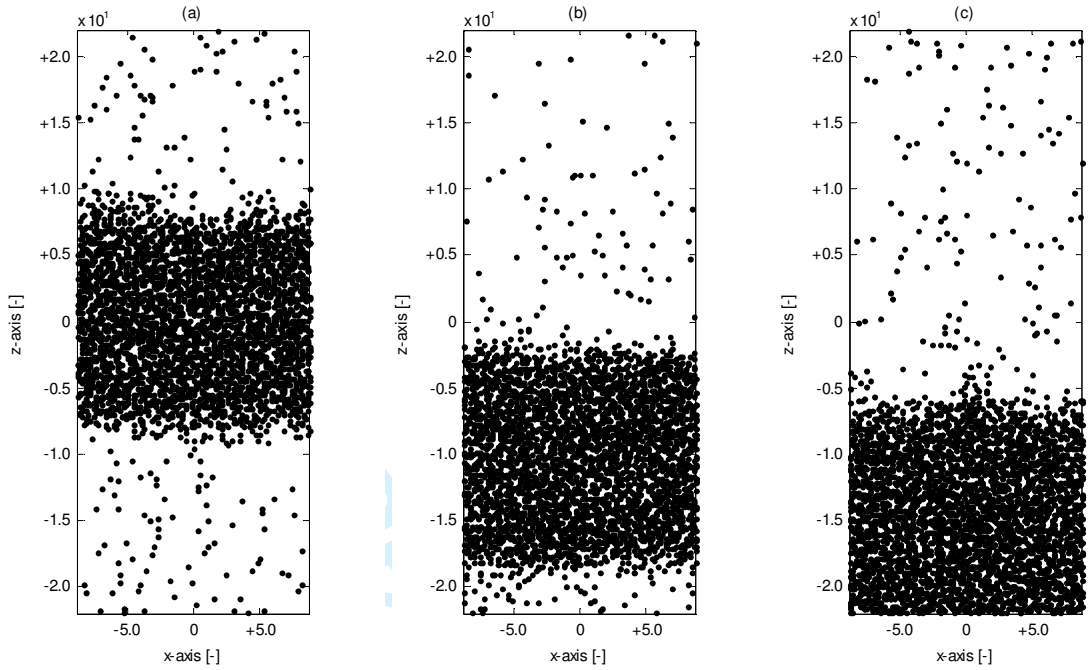

Figure 10: x-z-view of the initial state (a) at $t = 0$, of the intermediate state (b) at $t = 388$ and of the end state (c) at $t = 730$ of the particles in a two-phase system with a SRB condition at the bottom wall for MD simulation H. All values are in reduced Lennard-Jones units.

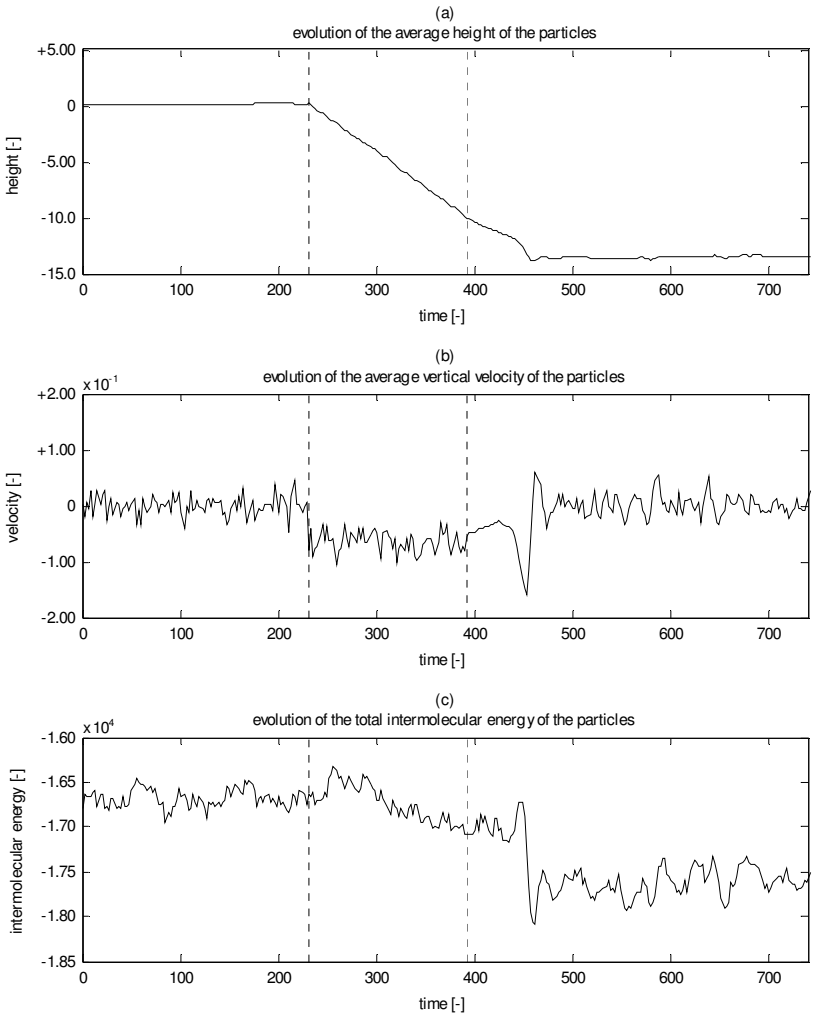

Figure 11: Evolution of the z-component of the position of the centre of mass (a), average vertical velocity (b) and total intermolecular energy (c) of the particles in a two-phase system with a SRB for MD simulation H. All values are in reduced Lennard-Jones units.